Summer 6-24-2022

SEDIMENTARY CHARACTERISTICS AND ASSOCIATED CARBON AND NUTRIENTS OF OVERBANK SEDIMENTS DEPOSITED DURING THE 2018, 2019, AND 2020 FLOODS IN EMBANKED FLOODPLAINS ALONG THE LOWER MISSISSIPPI RIVER NEAR NATCHEZ, MISSISSIPPI

Rachel Kelk

SEDIMENTARY CHARACTERISTICS AND ASSOCIATED CARBON AND NUTRIENTS OF OVERBANK SEDIMENTS DEPOSITED DURING THE 2018, 2019, AND 2020 FLOODS IN EMBANKED FLOODPLAINS ALONG THE LOWER MISSISSIPPI RIVER NEAR NATCHEZ, MISSISSIPPI

by

Rachel M. Kelk

A Thesis
Submitted to the Graduate School,
the College of Arts and Sciences
and the School of Biological, Environmental, and Earth Sciences
at The University of Southern Mississippi
in Partial Fulfillment of the Requirements
for the Degree of Master of Science

Approved by:

Dr. Franklin Heitmuller, Committee Chair
Dr. Kevin A. Kuehn
Dr. Bryan Piazza

August 2022

Published by the Graduate School

ABSTRACT

The Lower Mississippi River (LMR) experienced major floods in 2018, 2019, and 2020. Sediment deposition in the embanked floodplains during floods represent important storage and sequestration opportunities for carbon and nutrients from ~40% of the continental USA. This research aims to compare depositional thicknesses, organic matter (OM), carbon (C), nitrogen (N), phosphorous (P) concentrations, and grain sizes in floodplain sediments deposited by the combined 2018-19 floods to the 2020 flood along the LMR near Natchez, Mississippi. Greater depositional thicknesses in 2018-19 are best explained by their combined flood durations; the 2019 flood was the longest in recorded history. Slightly higher levels of OM in 2018-19 sediments indicate preservation favored by the extended duration of saturated conditions and/or increased organic productivity in the warm overbank water column during the later summer interval of the 2019 flood. Comparable concentrations of total C and N indicate that post-flood organic productivity rapidly converts available C and N to biological forms while diverse soil compositions and redox conditions equilibrate the remaining soil C & N to predictable levels commensurate with the floodplain setting (i.e., natural levees, backswamps). Low concentrations of P indicate removal of P from the soil to the flood waters as conditions become anaerobic and P is reduced and dissolution of clay- bound phosphates. Grain size values are dependent on flood duration, suspended sediment concentration, and floodplain environment.

ACKNOWLEDGMENTS

I am honored to thank the following people for all their help and support throughout these past two years in order to complete this thesis project to the fullest potential. First of all, I would like to share my gratitude to my advisor Dr. Franklin Heitmuller without who I would not have gotten this far, his guidance, steadfast support, encouragement, and knowledge made this project what it is today. I would also like to express my sincere gratitude to my committee members: Dr. Kevin Kuehn and Dr. Bryan Piazza. I wish to also extend my gratitude to Dr. Davin Wallace, Sarah Monica, and Saysha Sebren (lab equipment and guidance), Kent Ozment (sediment collection).

Much gratitude is needed for the to the School of Biological, Environmental and Earth Sciences and School of Ocean Sciences and Engineering at Stennis Space Center for equipment and instruments used. I also convey my gratitude to the Nature Conservancy for funding this project. I am also thankful to the research permit from St. Catherine Creek, U.S. Fish & Wildlife Service (field study), and the landowners Mr. Jerry Edwards and Mr. Eric Piazza.

Lastly, much love and dedication from my parents, without them behind me this project would not be to the caliber it is today.

TABLE OF CONTENTS

LIST OF TABLES

LIST OF ILLUSTRATIONS

LIST OF ABBREVIATIONS

LMR	Lower Mississippi River
OM	Organic Matter
C	Carbon
N	Nitrogen
P	Phosphorus
SCCNWR	St. Catherine Creek National Wildlife Refuge
USM	The University of Southern Mississippi
VRS	Virtual Reference Station

CHAPTER I - INTRODUCTION

The Lower Mississippi River (LMR) and its floodplain constitute a “textbook” example of a meandering river system that includes wide areas of various overbank deposits interrupted by present or former channel positions and deposits (Fisk 1944; Saucier 1994). Historically, sediment and nutrient delivery during floods from the LMR channel to its floodplain has supported intensive agriculture and the associated cities that flourished as a result, commonly at the expense of native riparian ecosystems. Conversion of the floodplain for agricultural purposes increased the need for flood control infrastructure (i.e., artificial levees), which reduced the connectivity of the current floodplain from its historic counterpart (Hudson and others 2008; Pongruktham and Ochs 2015). Rates of sediment deposition along the LMR are important for evaluation of flood hazards, because as more sediment is deposited, the area of overbank water storage is reduced, increasing flood risk (Heitmuller and others 2017). Sediment transported by the LMR is also vital for sustaining wetland ecosystems along the Louisiana Gulf Coast in the face of increasing relative sea levels and coastal storm impacts (Blum and Roberts 2009; Nittrouer and others 2012).

Along with sediments, flood pulses also transport nutrients to the floodplain (Spink and others 1998; Noe and Hupp 2000; Noe and Hupp 2005; Noe and others 2013;). These nutrients support and sustain ecological diversity and biological productivity (Spink and others 1998; Schramm and others 2009). Flooding events are beneficial from both a hydrological and biological standpoint. As fresh nutrients are regularly supplied by flooding events along the LMR, soil qualities improve for

agricultural uses and provide hydrologists a better understanding of the impact of upstream structures on downstream sediment transport (Pongruktham and Ochs 2015).

1.1 Research Questions

This proposed investigation aims to improve our understanding of sedimentary dynamics and associated carbon and nutrient exchanges in embanked floodplains along the LMR by addressing the following research questions:

1. Are depositional thicknesses, sedimentary characteristics, and carbon and nutrient levels in overbank sediments similar for different floods at the same locations in various floodplain settings? Specifically, how do these characteristics compare between the combined 2018-19 floods and the 2020 flood?
2. Do depositional thicknesses, sedimentary characteristics, and carbon and nutrient levels of floodplain deposits exhibit local (i.e., intrasite) variability? Does local variability change among different floodplain settings (i.e., natural levee, meander scroll, backswamp)?

It is anticipated that results and conclusions from this research will inform effective strategies to facilitate carbon and nutrient delivery and sequestration, and further enhance riparian habitats in the embanked floodplain.

CHAPTER II – LITERATURE REVIEW

2.1 Geologic Background

2.1.1 Lower Mississippi Valley

The Mississippi River is the third largest drainage basin in the world based on area (3,225,000 km^2) and the seventh largest in the world based on discharge (Horowitz 2010). The river flows 3770 km downstream from Lake Itasca, Minnesota, with contributions from watersheds within the Appalachian Mountains to the east and the Rocky Mountains to the west (Horowitz 2010; Kesel 2003). Roughly 75% of its discharge flows into the Gulf of Mexico southeast of New Orleans, Louisiana, and the remaining discharge is rerouted through the Old River Control Structure downstream from Natchez, Mississippi, where it joins the Red River to form the Atchafalaya River (Horowitz 2010).

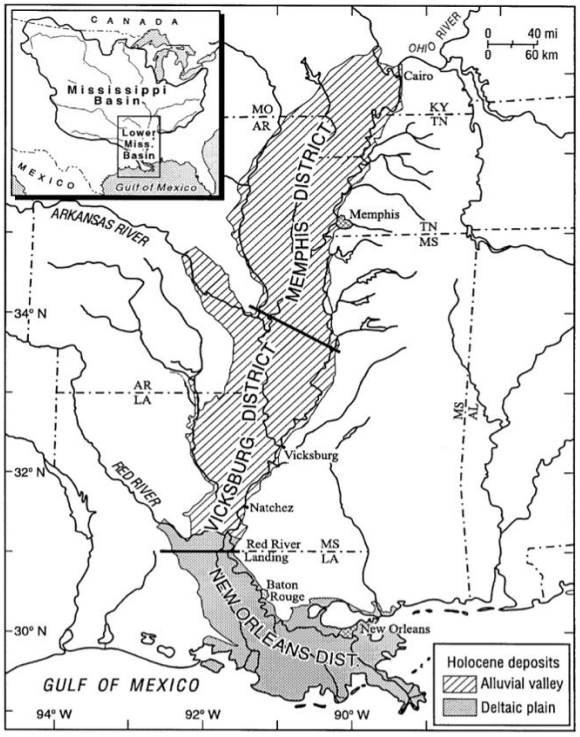

Figure 1.1 *Map of the Lower Mississippi River (Kesel 2003).*

For the purposes of this paper, the LMR is defined as the 1600 km segment (fig. 1.1) from the mouth of the Ohio River at Cairo, Illinois, down to the Gulf of Mexico (Kesel 2003). This extensive drainage basin includes a variety of land cover and use types including broad semi-arid to sub-humid grasslands, humid forests and woodlands, wetlands, floodplains, large-scale agricultural regions, and large urban

centers (Saucier 1994). Immense areas of natural and human-modified landscapes in the watershed result in dimensional and variable inputs of sediment, water, and both organic and inorganic constituents throughout the drainage network that flows into the main Mississippi River channel (Saucier 1994). Rates and quantities of these inputs to the LMR have changed considerably over both geological and historical timeframes (Saucier 1994; Schramm and others 2009; Horowitz 2010).

2.2 Relevant Scientific Concepts

2.2.1 Flood Pulse Concept

Before the anthropogenic, fluvial, and environmental considerations are further discussed, a general understanding of the flood pulse concept (Junk and others 1989) is given. Prior to the development of the flood pulse concept, flooding events were thought to be damaging to the floodplain (Benke and others 2000). However, the flood-pulse concept negated this theory; it explains the connection between the lateral exchange of water, nutrients, and biota from the main river channel to the floodplain (Junk and others 1989). Annual flood pulses are essential to biological productivity and ecological diversity in floodplains (Thorp and Delong 1994).

This concept is the backbone for understanding floodplain dynamics and the relationships between the hydrologic connectivity of the main channel to riparian habitats (Junk and others 1989; Stone and others 2017). In order for successful water management and restoration projects, a holistic understanding of the floodplain ecosystem is needed, including the transport of sediments and nutrients as well as the development of hydrogeomorphic features (Stone and others 2017). Without a general understanding of

the true benefits of flood pulses, artificial infrastructure can have severe negative side effects on floodplain ecosystems (Johnson and others 1995).

2.3 Anthropogenic Impacts

2.3.1 Flood Control Structures

Preceding flood-control modifications along the LMR, natural flooding inundated a large alluvial plain which spanned roughly 50 to 150 km resulting in a predictably widespread flood- pulse (Junk and others 1989). Large-scale human-induced changes were introduced to the LMR after 1920 (Kesel 2003) when Congress decreed that waterways must be maintained in a manner that provides navigation as well as protection from flooding in the alluvial valleys (Smith and Winkley 1996). However, the bulk of these structures were built in the 1930s after the great flood of 1927 by the U.S. Army Corps of Engineers (Smith and Winkley 1996). Since then, research has been conducted by the Corps with the hopes of making better and more effective structures (Smith and Winkley 1996).

Along the Mississippi River direct artificial controls include meander bend cutoffs, channel groins, bank revetments, earthen levees, floodways, and dams (Keown and others 1986). As a result of cutoffs, groins, and revetments, the river channel becomes straighter, deeper, and laterally more stable compared to its natural condition, which improves navigation and infrastructure along the river (Keown and others 1986). Stabilization of the river channel increases flow velocities, thus encouraging bed scouring at lower discharge stages (Kesel 2003).

Broad earthen levees have reduced the effective floodplain allowing for urban and agricultural infrastructure to move closer to the main channel (Keown and others 1986).

Furthermore, dams upstream in the watersheds of major tributaries such as the Arkansas, Missouri, and Tennessee Rivers unintentionally trap sediments from being delivered downstream (Keown and others 1986).

2.4 Fluvial Considerations

2.4.1 Sediment Transport

Development of flood-control structures upstream of the LMR has greatly reduced downstream sediment transport (Keown and others 1986; Horowitz 2010; Tockner and others 2010). Transport of approximately 400 million metric tons of sediments, the additions of revetments and reservoirs on the main channels of the Missouri and Arkansas Rivers, has reduced this rate almost 60% (Rus and others 2015). In general, the floodplains of large meandering river systems are often visualized as temporary storage for water during times of flooding and long-term storage for overbank sediments, so the reduction in sediment transport along the LMR has major impacts on the overall floodplain and its ecosystem (Kesel 2003; Kaase and Kupfer 2016). Furthermore, as more sediment is trapped by upstream control structures, less sediment is transported downstream leading to accelerated land loss along the coastal zone of Louisiana (Meade and Moody 2010; Heimann and others 2011). This land loss has become so extreme that diversion channels have been implemented to directly channel sediment down to the coast of Louisiana (Allison and Meselhe 2010).

Although there is a decrease in sediment transport rates because of upstream flood control structures, the sediments that are deposited along the floodplain are vertically accreting, thus reducing the overbank flood storage area (Hudson and others 2008). Deposition in floodplains is controlled by the suspended sediment concentration (SSC),

the sediment grain size, the overbank flow velocity, flood hydrograph characteristics (i.e., magnitude, duration) floodplain roughness (i.e., vegetation density and height relative to overbank water depths), and distance from the main channel (Asselman and Middelkoop 1995; Asselman and Middelkoop 1998; Bridge 2003). Overbank deposits modify the floodplain's topographic features and are strongly associated with differences in grain size, thus hydrologic connectivity between the channel and floodplains control sedimentation patterns and rates, thus diversifying morphologic characteristics and ecosystem processes (Kaase and Kupfer 2016). For example, as the water leaves the main channel and begins to inundate the floodplain, the first sediments that are likely to be deposited on the natural levees are sand-sized particles (Kesel and others 1974; Hudson and Heitmuller 2003). However, the further the water travels across the floodplain, the velocity of the flow decreases and remaining suspended sediments in the water column will begin to sink, depositing finer grained sediments (Kesel and others 1974; Kaase and Kupfer 2016).

Although much is known about geomorphic and sedimentary characteristics of the LMR alluvial valley (Fisk 1944; Saucier 1994; Aslan and Autin 1999; Hudson and Kesel 2000), research on overbank sediment deposition in the LMR alluvial valley is scarce. One of the few studies was conducted by Kesel and others (1974) after the infamous flood of 1973 (Heitmuller and others 2017). During this flood, the river was out of its banks for over two months, this prolonged duration allowed for more sediments of differing sizes to be deposited onto the floodplain (Kesel and others 1974). Grain sizes were coarsest along point bars and natural levees and finest in settings furthest from the main channel. In 2011, the highest recorded flood stage along the LMR embanked

floodplain near Natchez was responsible for deposition less than that documented for the 1973 flood (Heitmuller and others 2017). Compared to the results of Kesel and others (1974), most depositional sub-environments had a greater percentage of sand with less silts and clays being deposited during the 2011 flood (Heitmuller and others 2017).

2.4.2 Nutrient Sequestration

Seasonal inundation of floodplains acts as both a filter and a sink for nutrients (Schramm and others 2009). While flood pulses transport sediments from the main channel to the floodplain, they also transport carbon (C) and nutrients such as nitrogen (N) and phosphorus (P) (Noe and Hupp 2005; Noe and Hupp 2009; Noe and others 2013). Replenishment of nutrients to floodplains promotes ecological diversity and soil fertility, thus if sediment transportation is reduced, a concomitant reduction in nutrient supply to the floodplain is likely (Schramm and others 2009). The calculation of nutrient sequestration is a complex process that involves several variables including the amount of nutrients contained in soils, the amount used by fish, and the amount suspended in the water column and utilized by aquatic biota not including fish (Schramm and others 2009). Various investigations have attempted to quantify nutrient dynamics in floodplains such as Noe and Hupp (2005), which utilized the accumulated sediment along coastal plain rivers across the coastal plain of the Chesapeake Bay watershed to measure the nutrient content and further determine nutrient accumulation rates.

2.4.3 Soil

Floodplain soils serve as both a source and a sink for vital nutrients and provide the necessary conditions for multiple biogeochemical reactions that drive nutrient cycling (Noe and Hupp 2005; Schramm and others 2009). Specifically, floodplains can be sinks

for inorganic, organic, dissolved, or particulate fractions of both nitrogen and phosphorus (Tockner and others 1999; Noe and Hupp 2005). As the floodplain becomes inundated, the soils gradually become anaerobic, microorganisms reduce nitrate to nitrous oxide, and nitrogen is removed from the system as gas (Schramm and others 2009; Ochs and Shields 2019). Phosphorus availability also changes during periods of flooding (Schramm and others 2009; Schonbrunner and others 2012). During periods of inundation when the soils become anaerobic, phosphorus levels in the water column increase as a result of the reduction and dissolution of iron phosphates, the release of clay-bound phosphates, and the hydrolysis and dissolution of iron and aluminum phosphates (Schramm and others 2009).

Because nitrate is an anion, it is often subject to leaching during times when the soil is under aerobic conditions, therefore nitrate found within the floodplain soil was most likely deposited during flooding. As fresh nitrate-bearing water travels across floodplain soils, the longer the floodplain is inundated, the more nitrogen will be removed from the water by the soils. However, unlike soils being a sink for nitrogen, they are a source of phosphorus. Ferric iron-phosphates which are sequestered under aerobic conditions reduce to ferrous iron under anaerobic conditions which increases the amount of phosphorus available for plant uptake (Schramm and others 2009).

Previous studies have shown that floodplains are efficient traps for suspended solids, particulate organic matter, and nitrate (Tockner and others 1999; Noe and Hupp 2005; Noe and Hupp 2009; Noe and others 2013; Schramm and others 2009). Tockner and others (1999) conducted research along a floodplain segment of the Danube River, which indicated that riverine wetlands are effective nutrient sinks because nutrients

adsorbed to suspended river sediments are deposited. This idea is further supported in research done on floodplain sediments within the Atlantic Coastal Plain of the Chesapeake Bay watershed and in the forested wetlands of Difficult Run in Virginia (Noe and Hupp 2005; Noe and Hupp 2009; Noe and others 2013). These three studies compared the sediment accumulation rates of floodplain areas with differing land uses to determine the change in sequestration rates across different regions. Overall, they concluded that the land use has a large impact on sediment and nutrient retention rates and that hydrologic connectivity within the floodplain also has a major impact on these retention rates (Noe and Hupp 2005; Noe and Hupp 2009; Noe and others 2013).

2.5 Environmental Considerations

2.5.1 Alluvial-Deltaic Plain

Wetland habitats commonly found on alluvial-deltaic plains need regular intervals of inundation of nutrient-rich waters to maintain high levels of organic productivity, increase areas of fish spawning in low-velocity settings, and establish an abundance and diversity of species appropriate for the LMR floodplain ecoregion (Bayley 1991; Phelps and others 2015). Differences in flow velocity, inundation depth and duration, as well as sedimentation across the floodplain are evident among different features such as oxbow lakes, flood basin lakes, natural levees, ridge and swale topography, and backswamp environments (van der Most and Hudson 2018; Saucier 1994). These features should be taken into consideration for quantification of sedimentation rates and nutrient sequestration and should be further considered to understand the impact of flood control structures (Heitmuller and others 2017; Keown and others 1986; Kesel 2003).

2.5.2 Coastal Zone and Gulf of Mexico

Coastal and marine environments of the northern Gulf of Mexico are substantially impacted by sediment and nutrient dynamics of the LMR (Dokka 2006). Land loss in coastal Louisiana, wetland conversion to open water bodies, and salt-water encroachment into previously freshwater habitats are all associated with a combination of eustatic sea level rise, ground surface subsidence, and a decrease in sediment transport from the LMR (Dokka 2006; Blum and Roberts 2009).

Offshore, an annual hypoxic zone in the Gulf of Mexico is primarily caused by algal blooms supported by the high levels of dissolved nutrients transported by the LMR (Rabalais and others 2002). Onshore, one of the primary benefits of wetland and riparian lakes is their ability to absorb and sequester dissolved nutrients from the flood waters into the sediments and soils, thus facilitating nutrient uptake by organisms or conversion via mineralization (Mitsch and Day 2006). When the floodplain is unable to sequester dissolved nutrients, they are flushed downstream to the Gulf of Mexico causing the algal blooms which create and sustain the hypoxic zone (Rabalais and others 2002). Developing a holistic view of the interactions and dynamics of sediments and nutrients transported by the LMR would shed a light on how to best handle these issues today.

CHAPTER III- METHODS

3.1 Field Collection

In October 2019, researchers from The University of Southern Mississippi (USM), in collaboration with the Saint Catherine Creek National Wildlife Refuge (SCCNWR) and The Nature Conservancy, measured depositional thicknesses and collected 121 sediment samples from 48 sites in representative overbank settings in the embanked floodplain of the LMR following the major 2018 and 2019 floods (fig. 3.1).

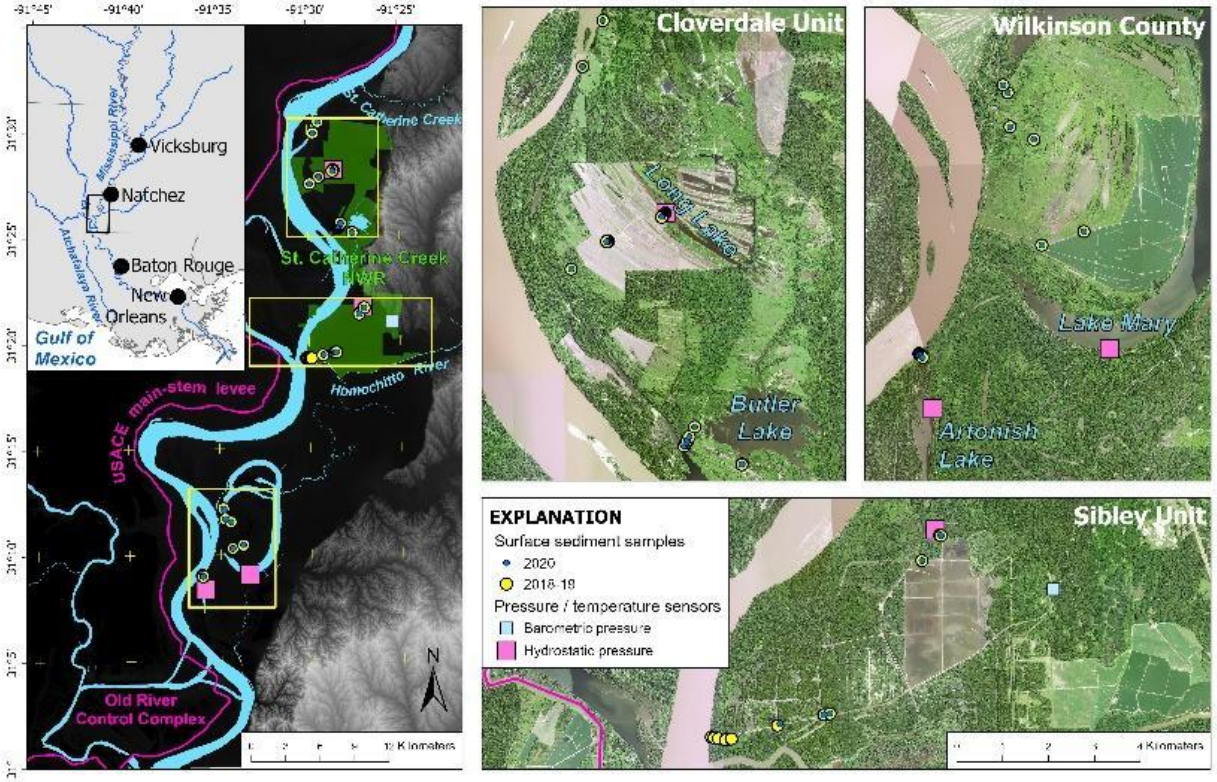

Figure 3.1 *Map of study area down river of Natchez, Mississippi (MS) with focused maps of the Cloverdale Unit sites, the Wilkinson Counties sites, and the Sibley unit sites for the 2018-2019 and 2020 floods.*

Identification of the flood deposits was possible by observing either an oxidized layer or leaf litter beneath the fresh sediments. In sandy samples, flood deposits were delineated by observing a relatively dark, fine-grained drape beneath the overlying

sediment layer. The 2018-19 flood deposits were combined due to the minimal time that was available for oxidation rinds to form and the rising limb of the 2019 flood preceded leaves dropping in the fall and winter. Three thickness measurements were taken and averaged at each site. A 60 cm × 60 cm sampling grid was used to aid in sampling at multiple locations. At sites where the grid was used, four samples were collected. The sampling grid was placed in an area of low vegetation, once the first sample was collected the grid was 'flipped' forward and another sample collected, then the grid was 'flipped' to the right and finally 'flipped' back down for a total of four samples collected. Upon collection, samples were placed in coolers and then a freezer to preserve the in-situ carbon and nitrogen values. A Trimble GeoXH 6000 GPS (centimeter edition) and Zephyr Model 2 antenna mounted to a survey pole were used to collect position and elevation data at each site; accuracies were improved by real- time connection to the Mississippi Virtual Reference Station (VRS) network and differential correction using Trimble Pathfinder Office software. Additionally, overbank water level and temperature data were retrieved from four previously installed Onset Hobo sensors, which were subsequently redeployed for an additional monitoring period.

In November 2020, sediment samples deposited by the major 2020 flood were measured for thickness and recollected from the same sites (if accessible), which were located by using the Trimble GeoXH GPS to navigate to site positions. Upon collection, samples were placed in coolers and then a freezer to preserve the in-situ carbon and nitrogen values. When the 2020 samples were returned to the lab, they were placed in a refrigerator that was kept at six degrees above freezing, which may alter the in-situ nutrient values.

Some sites that were visited in 2019 were unable to be reassessed in 2020 on account of a washed-out drainage culvert, which was unable to be safely crossed. Sample SCCNWR 503 was not collected at the same location but was collected in close proximity to the previous site. Sites SCCNWR 055, 501, 056, 057, and 502 were not resampled in 2020. Two sites on natural levees along Carthage Point Road did not have observable evidence of overbank sediments associated with the 2020 flood, nevertheless samples were collected from the surface. Finally, overbank water level and temperature data for the 2020 flood were downloaded from the four sensors that were redeployed during the 2019 visit. The field data were recorded at 4-hour intervals, which were later processed to daily mean values for graphing purposes.

3.2 Laboratory Analysis

Sediment samples were split into smaller subsamples; one was freeze-dried using a lyophilizer for carbon and nutrient analysis and the remaining sample was used for magnetic susceptibility, grain size, and organic matter. Freeze-dried samples were analyzed for carbon (C) and nitrogen (N) using a Costech elemental combustion analyzer, and total phosphorus (P) was determined using a SEAL AA3 flow-injection nutrient analyzer. Particle size in millimeters were determined using a Malvern Masterizer 3000 For the other subsample, magnetic susceptibility will be analyzed using a Bartington MS-2B sensor and MS-3 meter, and percent organic matter was determined using a muffle furnace for loss on ignition.

The C and N analysis required 20 milligrams of the dried sediment to be measured out and encapsulated in tin cups. Quality control samples were measured out to ~ 0.50 milligrams of atropine. After the initial standards were run, a quality control

sample was analyzed after every twelve samples of sediment. Standards of atropine were measured out to 0.25, 0.50, 0.75, and 1.0 respectively for each C and N analysis run.

Loss on ignition was completed in sets of 50 samples. First, crucibles were wiped out and placed in an oven for two hours at 105°C. The crucibles were then cooled in a desiccator and an empty weight was measured while the crucibles were in the desiccator. Dried crucibles were filled one-quarter their volume with sediment left over from the C and N analysis. The partly filled crucibles were placed back in the oven for two more hours, cooled and weighed again, and placed in the muffle furnace for four hours at 500°C.

Total phosphorus (P) analysis was initiated by weighing out roughly 250 mg of dried sediment into glass tubes that were capped with aluminum foil. The tubes were then placed in the muffle furnace at 500°C for four hours and left to cool overnight. Standard P solutions were created by dissolving 0.2197 grams of oven-dried potassium dihydrogen phosphate (KH_2PO_4) in a 1000 ml flask and diluted to one liter. After this stock was mixed, five standard solutions were made (Table 1).

Table 3.1 *Standard solutions used for phosphorus concentration measurements.*

PO_4 Concentrations µg/L	Amount of 1.0N HCL (ml)	Amount of Phosphorus Standard (ml)
0	125	0.0
5	125	0.5
10	125	1.0
30	125	3.0
50	125	5.0
100	125	10.0
150	125	15.0
***High standard (15) in 250 ml solution**	**625**	**75.0**

Sample preparation included 5 ml of 1.0 M HCl was added to the muffled samples and mixed well. The tubes were then placed in a boiling water bath for thirty minutes. Once cooled, 5 ml of distilled water was added bringing the sample volume to 10 ml. After further cooling and settling, 10 ml of distilled water was added to a pre-labeled Falcon polypropylene tube using a repeater pipet. Next, 50 µl of sample was added to the 20 ml of distilled water giving the samples a dilution factor of 401/1 for extract concentration which was refrigerated until analysis.

Grain size analysis was completed using a Malvern Mastersizer 3000. Prior to analysis, roughly three grams of dried and crushed sediment were placed in a 20 ml vial, then a 3:1 ratio of distilled water to 5% solution of sodium hexametaphosphate was added and left to sit for 48 hours. After 48 hours, the samples were sieved into a beaker using a 500 µm sieve. Samples were then brought into suspension and pipetted into the Malvern until obscuration was in range. Grain sizes were placed into statistical groups: D_{10}, D_{16}, D_{50}, D_{84}, and D_{90}. Each group is percentiles representative of different grain sizes for a sample. Once the sample was finished running, the Malvern was rinsed with two gallons of water between each sample run.

Magnetic susceptibility of the samples was analyzed using a Bartington MS2B dual- frequency sensor and a MS3 meter. Mass-based measurements were recorded in SI units, 10 g of sample were measured out into the Bartington specific plastic container and run through Bartington's analytical software.

3.3 Statistical Analysis

Results from the statistical analyses, described below, will be contextualized with flood hydrograph data, overbank water levels from the sensors, and measured

depositional thicknesses during the two floods. These analyses will be conducted using RStudio. Prior to all statistical testing, a Shapiro- Wilkes test for normality was conducted and determined that all variables were non-normally distributed. Due to this abnormality, a log transformation was performed on the data.

3.3.1 Flood Comparison

This experiment compares five factors across two treatment groups. These five factors are sediment grain size, organic matter content, carbon content, nitrogen content, and phosphorus content. The two treatment groups are the 2018-2019 flood samples and the 2020 flood samples. The dependent variables are the five factors listed above and the independent variable is the flood sediment deposition for each flood. This experiment can be replicated by recollecting samples from the same locations on the floodplain and reanalyzing the sediments. To compare these two floods, a Wilcoxon paired-sample nonparametric test was used. The following null hypotheses were tested:

1. The mean difference in sediment grain size between the 2018-2019 floodplain sediments and the 2020 floodplain sediments is equivalent to zero.
    a. The D_{10}, D_{16}, D_{50}, D_{84}, and the D_{90} are the grain sizes being collected to complete the statistical comparison.
2. The mean difference in the organic matter content between the 2018-2019 floodplain sediments and the 2020 floodplain sediments is equivalent to zero.
3. The mean difference in the carbon content between the 2018-2019 floodplain sediments and the 2020 floodplain sediments is equivalent to zero.

4. The mean difference in the nitrogen content between the 2018-2019 floodplain sediments and the 2020 floodplain sediments is equivalent to zero.
5. The mean difference in the phosphorus content between the 2018-2019 floodplain sediments and the 2020 floodplain sediments is equivalent to zero.

If I failed to reject the previously stated null hypotheses, I would conclude that there is no significant difference in the mean factor values of the 2018-2019 floodplain sediments and the 2020 floodplain sediments. I would further conclude that the two floods had different durations and timings.

If I rejected the above null hypotheses, I would conclude that there is a significant difference in the mean factor values of the 2018-2019 floodplain sediments and the 2020 flood plain sediments. I would then further conclude that the two floods had different floodplain conditions.

Because five sites were inaccessible in 2020 and multiple samples from those locations were collected in 2019, those samples will only be used to test for intrasite variability and will not be used in the above paired sample test.

3.4 Intrasite Variation

Intrasite variability compared the same five experimental factors as the flood comparison (listed above), however, the treatment groups will be individual sites rather than overall flood deposits from the 2018-2019 flood and the 2020 flood. These individual sites had four samples collected using the 60 cm x 60 cm sampling grid. To determine intrasite variation, coefficients of variation were calculated and then a two-way analysis of variance (ANOVA) was run. The following null hypotheses were tested:

1. Differences in mean grain size values are equivalent to zero between samples from each site.
2. Differences in mean organic matter content are equivalent to zero between samples from each site.
3. Differences in mean carbon content are equivalent to zero between samples from each site.
4. Differences in mean nitrogen content are equivalent to zero between samples from each site.
5. Differences in mean phosphorus content are equivalent to zero between samples from each site.

Should the previously stated null hypothesis be rejected, I would conclude that the mean values at each site are not the same and therefore there is intra site variability.

3.5 Intersite Variation

Intersite variability was also compared the same five experimental factors as the yearly comparison and intrasite variation, however, the treatment groups were the three floodplain environments (natural levee, meander scroll, and backswamp). To determine intersite variation, a two-way ANOVA was run on the raw data values. The following null hypotheses were tested:

1. Differences in mean grain size values are equivalent to zero between samples from each environment.
2. Differences in mean organic matter content are equivalent to zero between samples from each environment.

3. Differences in mean carbon content are equivalent to zero between samples from each environment.
4. Differences in mean nitrogen content are equivalent to zero between samples from each environment.
5. Differences in mean phosphorus content are equivalent to zero between samples from each environment.

Should the previously stated null hypothesis be rejected, I would conclude that the mean values at each site are not the same and therefore there is intersite variability.

CHAPTER IV– RESULTS

4.1 Field and Laboratory Results

Floodplain sedimentation thicknesses for the 2018-19 flood ranged from 12 mm to 1.4 meters with average thicknesses of 181 mm for natural levees, 30 mm for meander scrolls, and 108 mm for backswamps. Depositional thicknesses for the 2020 flood ranged from 3.3 to 162 mm with average thicknesses of 101 mm for natural levees, 10 mm for meander scrolls, and 28 mm for backswamps (fig. 4.1).

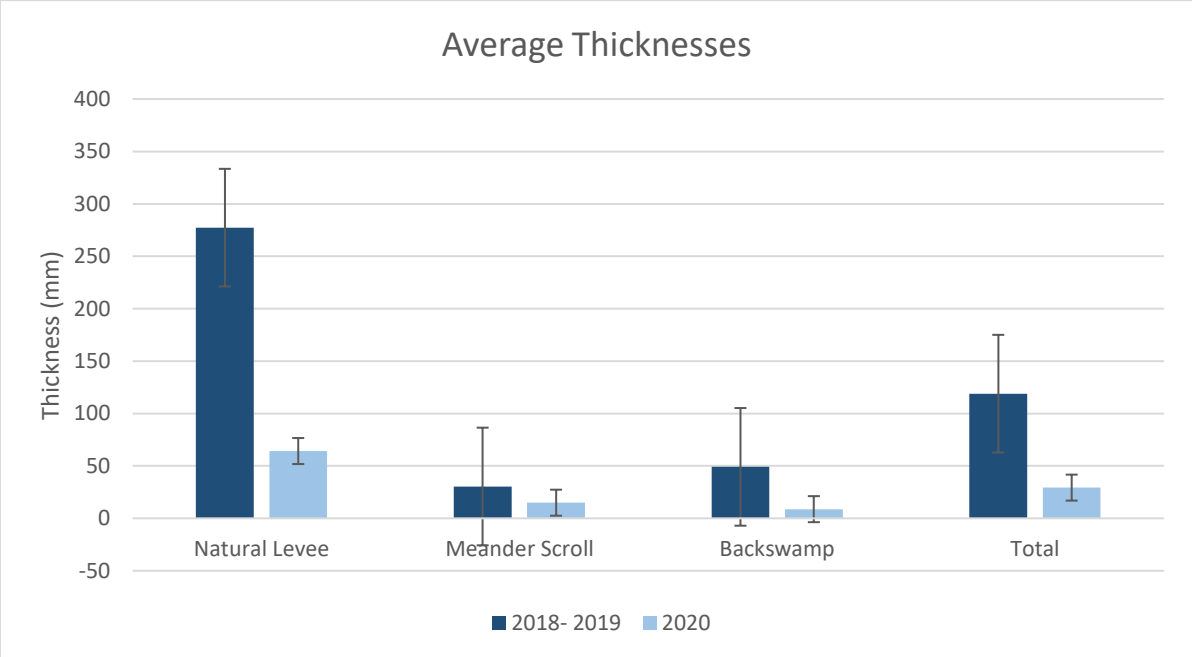

Figure 4.1 *Average depositional thicknesses compared between the 2018-19 flood deposits and the 2020 flood deposits.*

For 2018-19, the D50 grain size value averaged 136.85 µm, for natural levees, 5.19 µm for meander scrolls and 9.38 µm for backswamps. For 2020, grain size averaged 173.68 µm for natural levees, 11.54 µm for meander scrolls, and 14.34 µm for

backswamps (fig. 4.2).

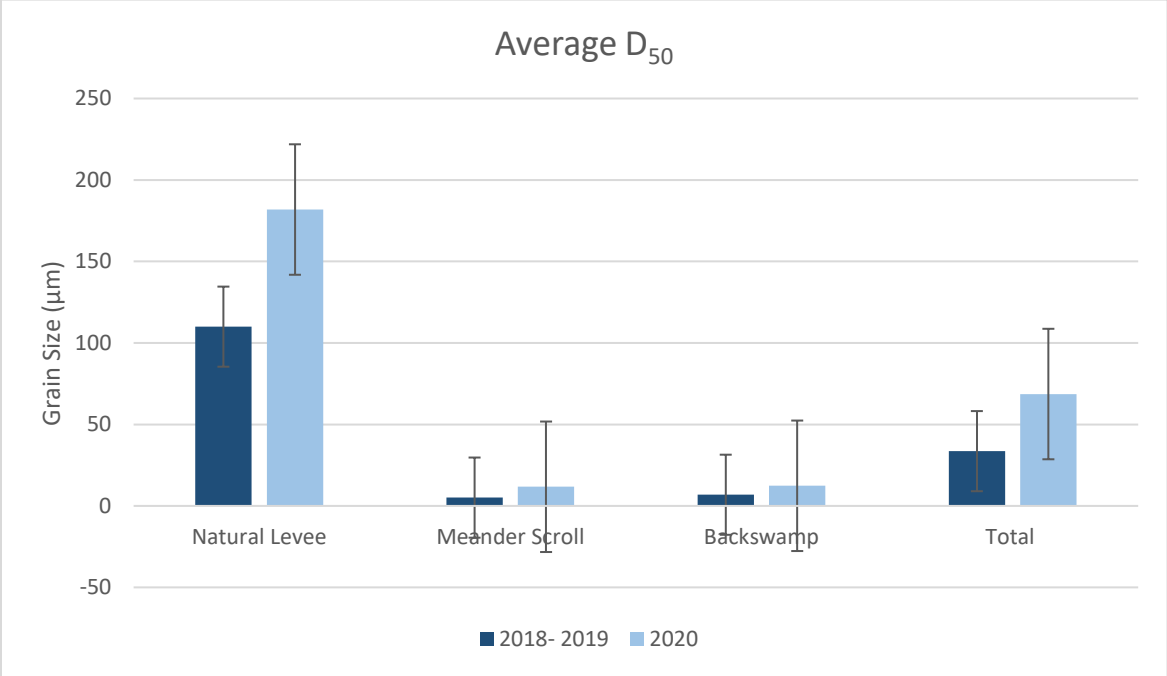

Figure 4.2 *Average D50 values (in microns) compared between the 2018-19 flood sediments and the 2020 flood sediments.*

For 2018-19, organic matter (OM) content ranged from 0.11–4.38% with averages of 0.68% for natural levees, 2.82% for meander scrolls, and 2.11% for backswamps. For 2020, OM content ranged from 0.15–3.32% with averages of 0.32% for

natural levees, 2.26% for meander scrolls, and 2.09% for backswamps (fig. 4.3).

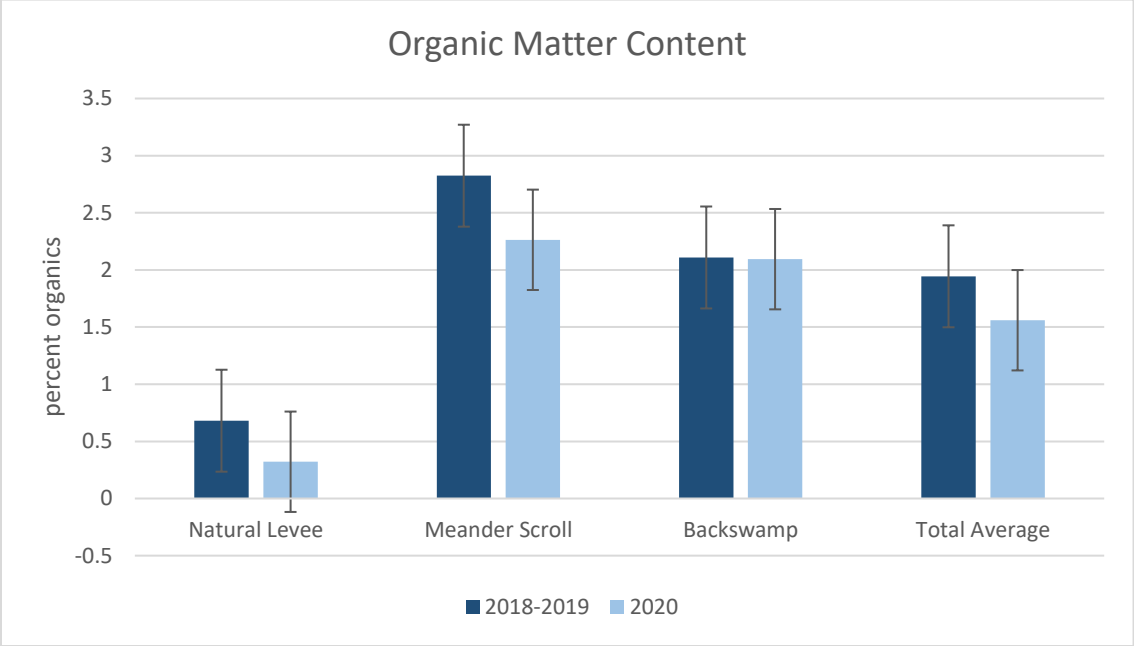

Figure 4.3 *Average organic matter percentages compared between the 2018-19 and 2020 flood sediments.*

For 2018-19, total C and N concentrations (by weight) averaged 2.78% and 0.23%, respectively, with averages of 0.51% C and 0.02% N for natural levees, 3.36% C and 0.28% N for meander scrolls, and 2.41% C and 0.20% N for backswamps. For 2020, total C and N concentrations averaged 2.86% and 0.23%, respectively, with averages of 0.40% C and 0.02% N for natural levees, 3.35% C and 0.27% N for meander scrolls, and 2.62% C and 0.22% N for backswamps (fig. 4.4 & 4.5).

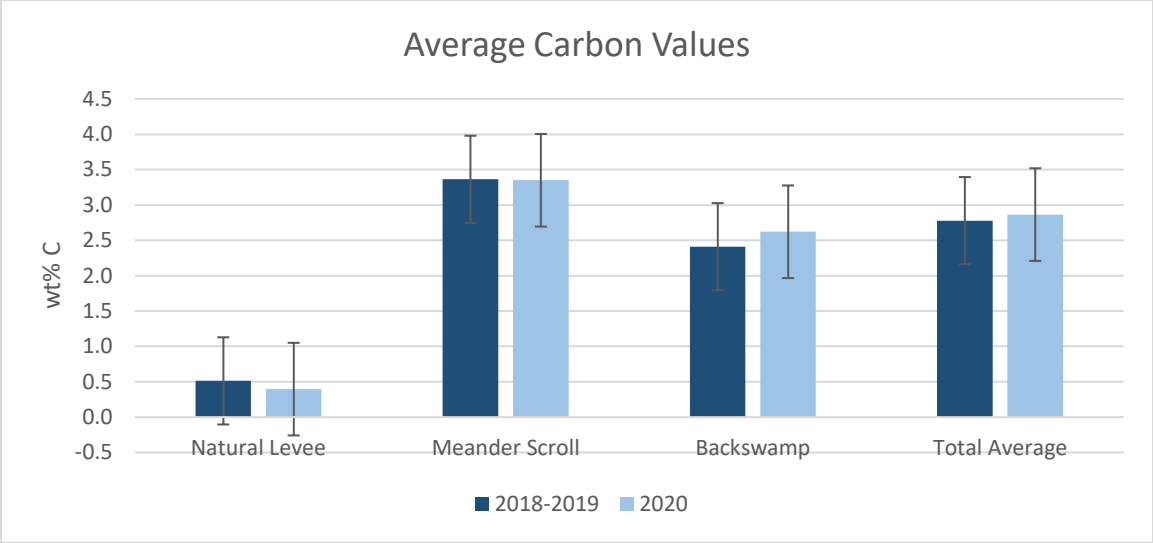

Figure 4.4 *Average weight percent of carbon compared between the 2018-19 and 2020 floodplain sediments.*

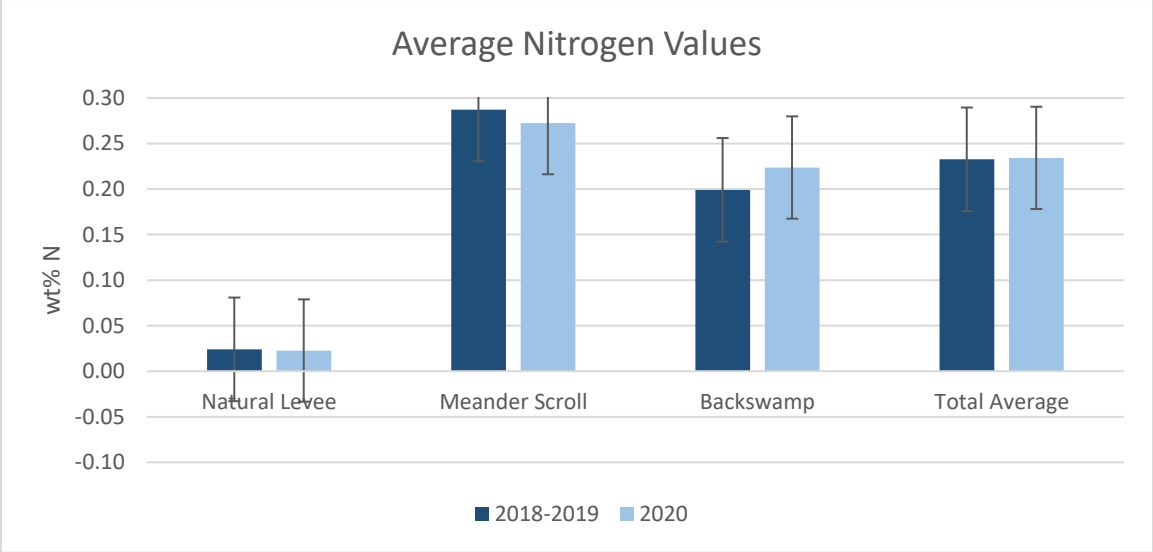

Figure 4.5 *Average weight percent of nitrogen compared between the 2018-19 and 2020 floodplain sediments.*

For 2018-19, total P concentrations by weight ranged from 0.007% to 0.084% and averaged 0.0405% for natural levees, 0.090% for meander scrolls, and 0.075% for backswamps. For 2020, total P averaged 0.019% for natural levees, 0.092% for meander scrolls, and 0.065% for backswamps (fig. 4.6).

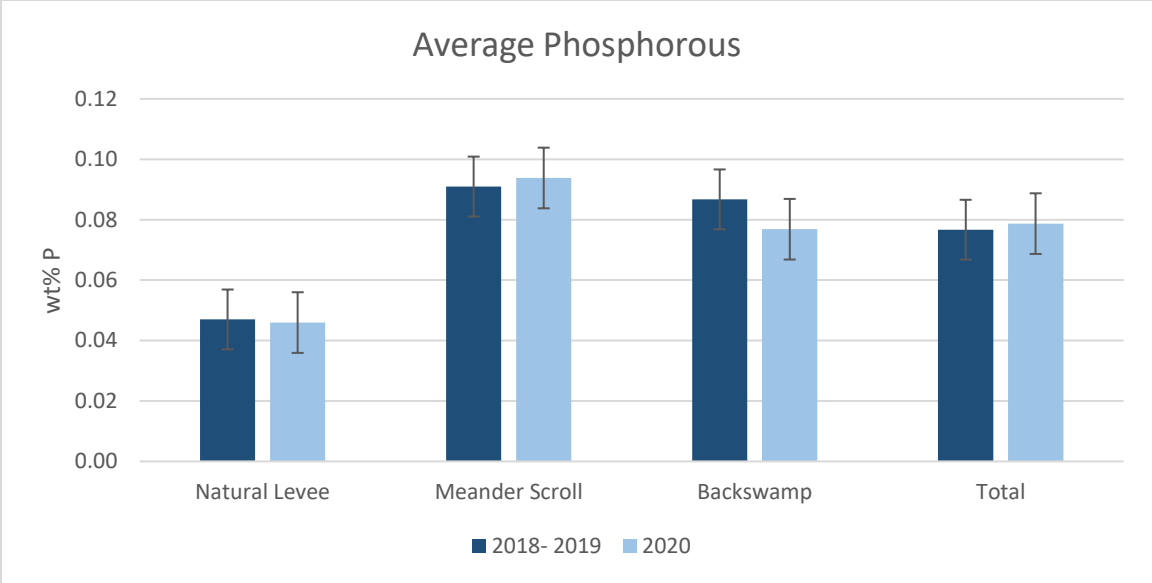

Figure 4.6 *Average weight percent of phosphorus compared between the 2018-19 and 2020 floodplain sediments.*

Prior to any statistical analysis, a Shapiro- Wilkes test for normality was performed on each parameter and determined that none of the variables were normally distributed. Once the assumption of normality was rejected a log transformation was performed on each parameter. The log transformation did not improve normality so for the flood comparison analysis, a nonparametric Wilcoxon signed rank test was performed to test the null hypothesis that differences in mean for each parameter was equivalent to zero (table 4.1 & 4.2). Wilcoxon signed rank test was chosen due to it being a good alternative to the t- test to test whether there is a difference in mean between two populations, in this case the two flood years.

Table 4.1 *Recorded P- values for the Wilcoxon signed rank test (P< 0.05) for carbon, nitrogen, phosphorus, and organic matter. This test determined whether there was a difference in the mean between the 2018-19 flood sediments and the 2020 flood sediments. Bolded values indicate no difference in the mean between the two floods and values of P< 0.05 indicate a statistical difference between the years. '*' certain phosphorus values were measured as zero so this value may be incorrect*

	All Sediments	*Natural Levee*	*Meander Scroll*	*Backswamp*
C	***0.5699***	***0.1094***	***0.7793***	***0.9375***
N	*<0.05*	***0.2807***	*<0.05*	*< 0.05*
P	***0.372***	***0.4375***	***0.7451***	***0.375***
OM	*<0.05*	***0.1094***	*< 0.05*	***0.9375***

Table 4.2 *Recorded P- values for the Wilcoxon signed rank test (P< 0.05) for grain size percentiles. This test determined whether there was a difference in the mean between the 2018-19 flood sediments and the 2020 flood sediments. Bolded values indicate no difference in the mean between the two floods and values of P< 0.05 indicate a statistical difference between the years.*

	All Sediments	*Natural Levee*	*Meander Scroll*	*Backswamp*
D_{10}	*< 0.05*	***0.5469***	*< 0.05*	*< 0.05*
D_{16}	*< 0.05*	***0.7422***	*< 0.05*	*< 0.05*
D_{50}	*< 0.05*	***0.9453***	*< 0.05*	*< 0.05*
D_{84}	*< 0.05*	***0.3125***	*< 0.05*	***0.2188***
D_{90}	*< 0.05*	***0.1953***	*< 0.05*	***0.1563***

For the intrasite variability, coefficients of variation were calculated for all sites that had four replicates collected using the 60cm × 60cm sampling grid, then a two- way

analysis of variance (ANOVA) was run on those coefficients of variation to test for interactions between flood plain environment and the flood year (table 4.3 & 4.4).

Table 4.3 Recorded Pr> F values calculated from the two- way ANOVA for intrasite variability for carbon, nitrogen, phosphorous, and organic matter. This test determined whether there was a difference in the mean between the replicate samples collected at each site. Bolded values indicate no difference in the mean between the two floods and values of < 0.05 indicate a statistical difference between the years. '' certain phosphorous values were measured as zero so this value may be incorrect.*

	C	*N*	*P**	*OM*
Year	***0.730***	***0.160***	*<0.05*	***0.470***
Environment	***0.447***	***0.135***	***0.36711***	***0.780***
Year & Environment	***0.795***	***0.436***	***0.93151***	***0.599***

Table 4.4 *Recorded Pr> F values calculated from the two- way ANOVA for intrasite variability for grain size percentiles. This test determined whether there was a difference in the mean between the replicate samples collected at each site. Bolded values indicate no difference in the mean between the two floods and values of < 0.05 indicate a statistical difference between the years.*

	D10	*D16*	*D50*	*D84*	*D90*
Year	***0.337***	***0.466***	***0.159***	*<0.05*	*<0.05*
Environment	***0.311***	***0.390***	***0.434***	***0.9623***	***0.6863***
Year & Environment	***0.573***	***0.618***	***0.557***	***0.0879***	***0.0937***

Further testing was performed to represent intersite variability to determine if there was a statistical difference in samples collected across environments (i.e., backswamps, meander scrolls, natural levees). This two- way ANOVA was run using the

raw averages from each site to test for interaction between environment and flood year (table 4.5 & 4.6).

Table 4.5 *Recorded Pr> F values calculated from the two- way ANOVA for intersite variability for carbon, nitrogen, phosphorous, and organic matter.*

This test determined whether there was a difference in the mean between the sites at each environment. Bolded values indicate no difference in the mean between the two floods and values of < 0.05 indicate a statistical difference between the years.

Intersite	*C*	*N*	*P*	*OM*
Year	***0.898***	***0.888***	***0.720***	***0.426***
Environment	*<0.05*	*<0.05*	*<0.05*	*<0.05*
Year & Environment	***0.712***	***0.713***	***0.875***	***0.728***

Table 4.6 *Recorded Pr> F value recorded from the two- way ANOVA for intersite variability for grain size percentiles. This test determined whether there was a difference in the mean between the sites at each environment. Bolded values indicate no difference in the mean between the two floods and values of < 0.05 indicate a statistical difference between the years.*

Intersite	*D10*	*D16*	*D50*	*D84*	*D90*
Year	***0.577***	***0.512***	***0.385***	***0.0785***	*<0.05*
Environment	*<0.05*	*<0.05*	*<0.05*	*<0.05*	*<0.05*
Year & Environment	***0.670***	***0.668***	***0.664***	***0.737***	***0.8527***

4.2 Other Data

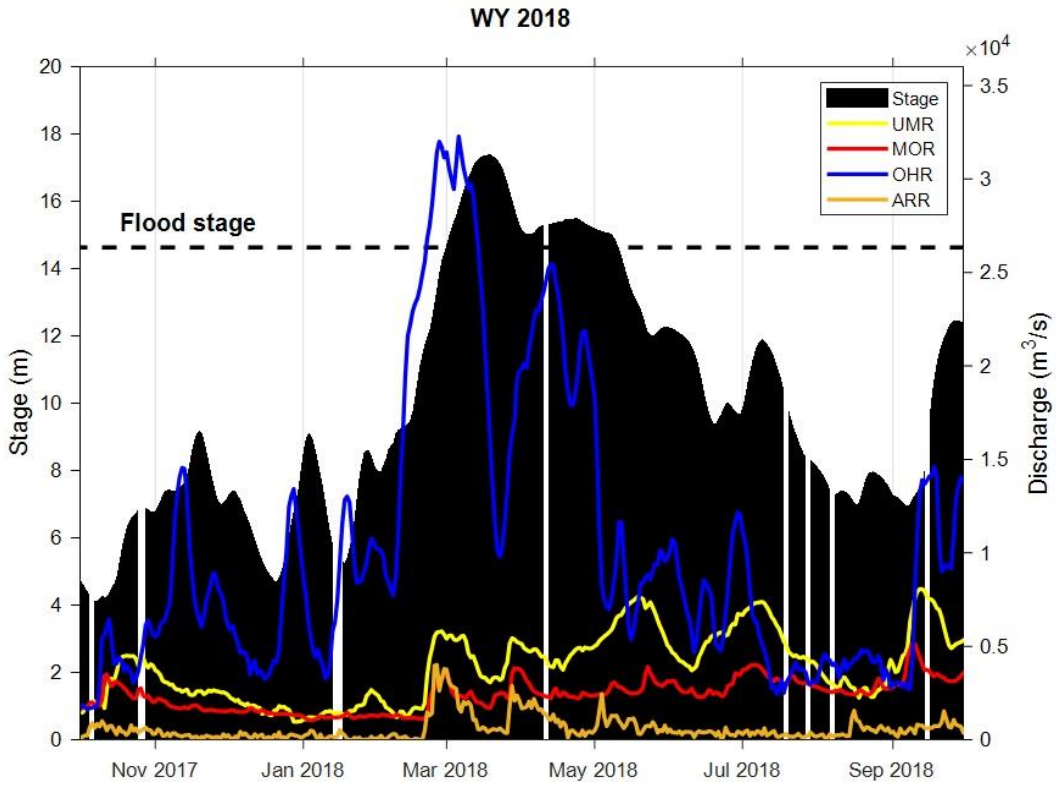

Figure 4.7 *Flood hydrograph for the 2018 water year where the black represents flood stage, the yellow represents the Upper Mississippi River, the red represents the Missouri River, the blue represents the Ohio River, and the orange represents the Arkansas River.*

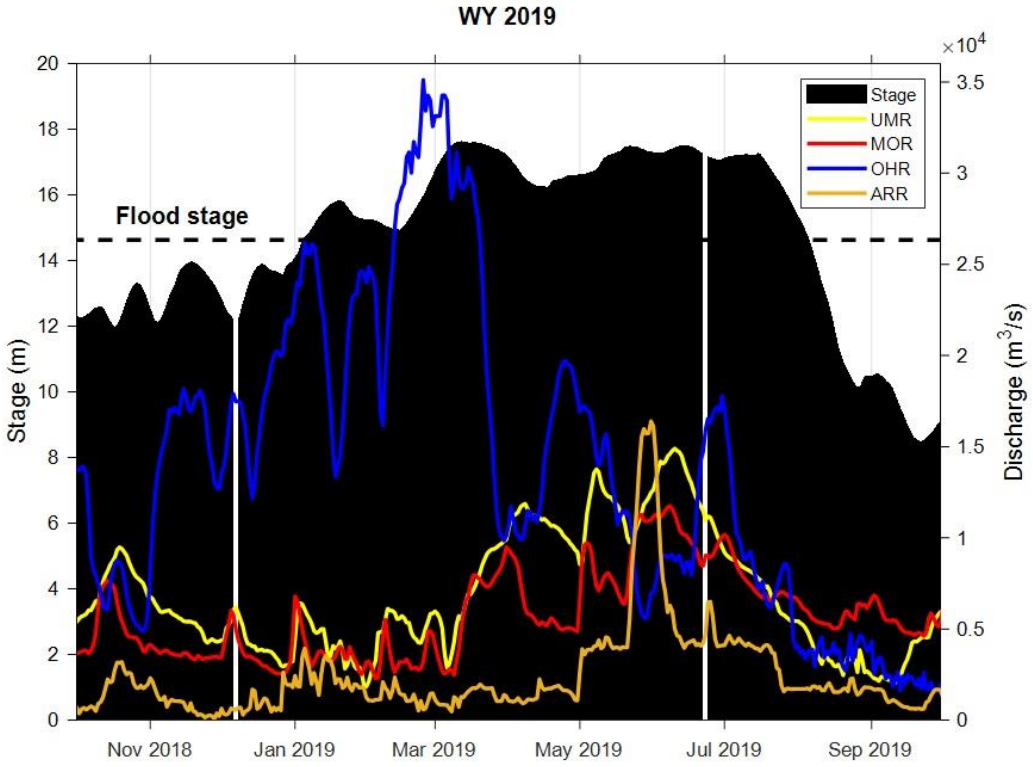

Figure 4.8 *Flood hydrograph for the 2019 water year where the black represents flood stage, the yellow represents the Upper Mississippi River, the red represents the Missouri River, the blue represents the Ohio River, and the orange represents the Arkansas River.*

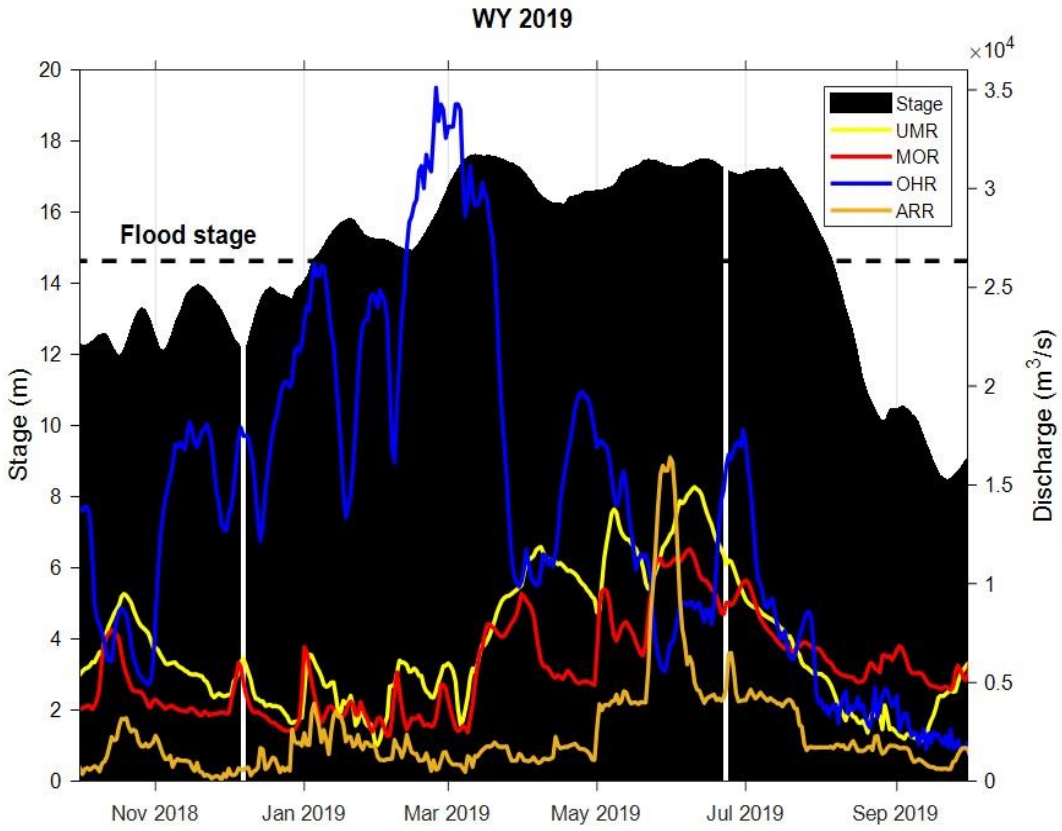

Figure 4.8 *Flood hydrograph for the 2019 water year where the black represents flood stage, the yellow represents the Upper Mississippi River, the red represents the Missouri River, the blue represents the Ohio River, and the orange represents the Arkansas River.*

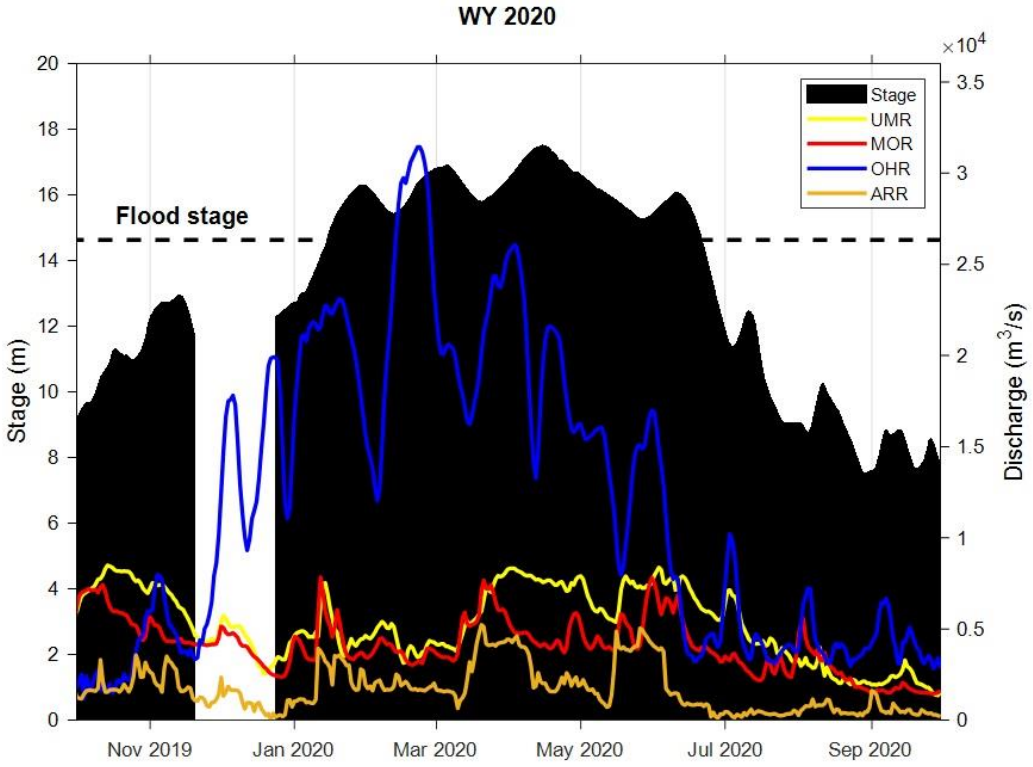

Figure 4.9 *Flood hydrograph for the 2020 water year where the black represents flood stage, the yellow represents the Upper Mississippi River, the red represents the Missouri River, the blue represents the Ohio River, and the orange represents the Arkansas River.*

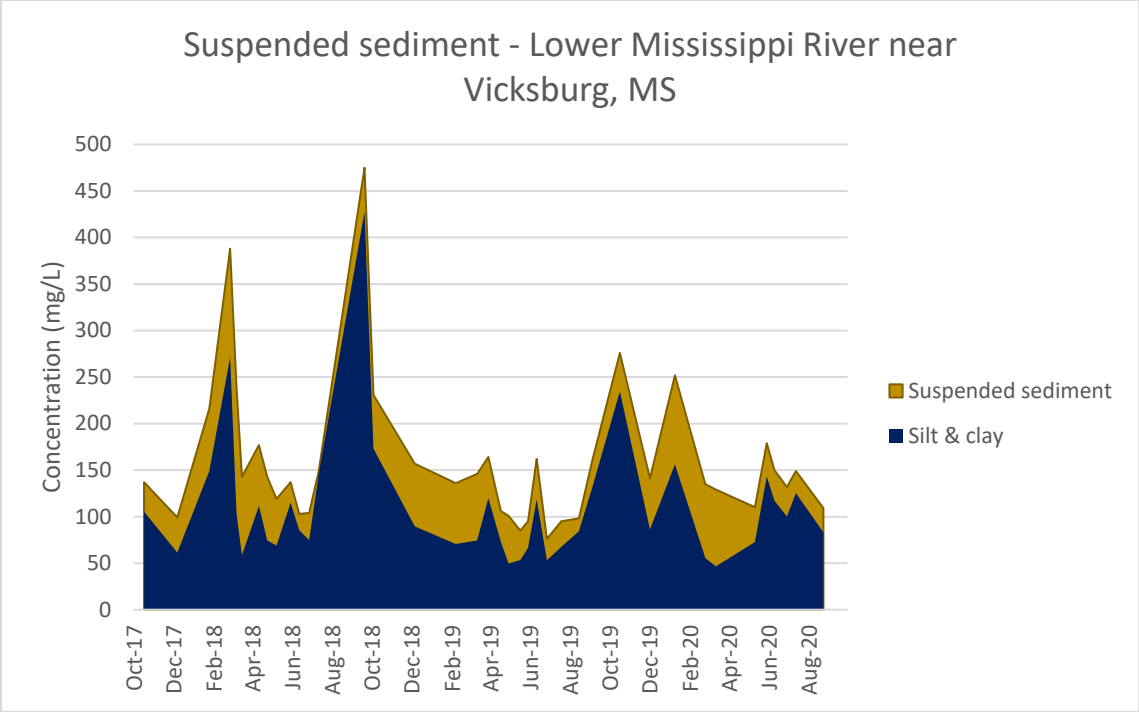

Figure 4.10 *Suspended sediment concentrations. Water data taken from the USGS (accessed April 2022).*

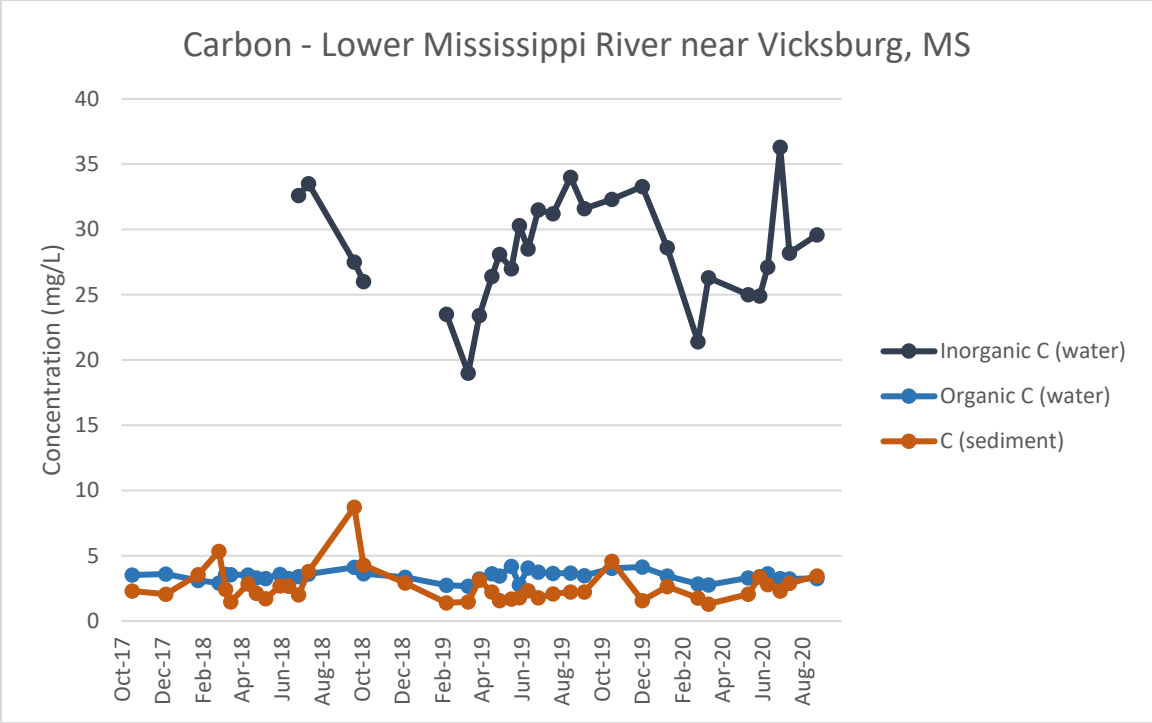

Figure 4.11 *Concentration of carbon within the water column from the Vicksburg, MS water collection point. Data taken from the USGS (accessed April 2022).*

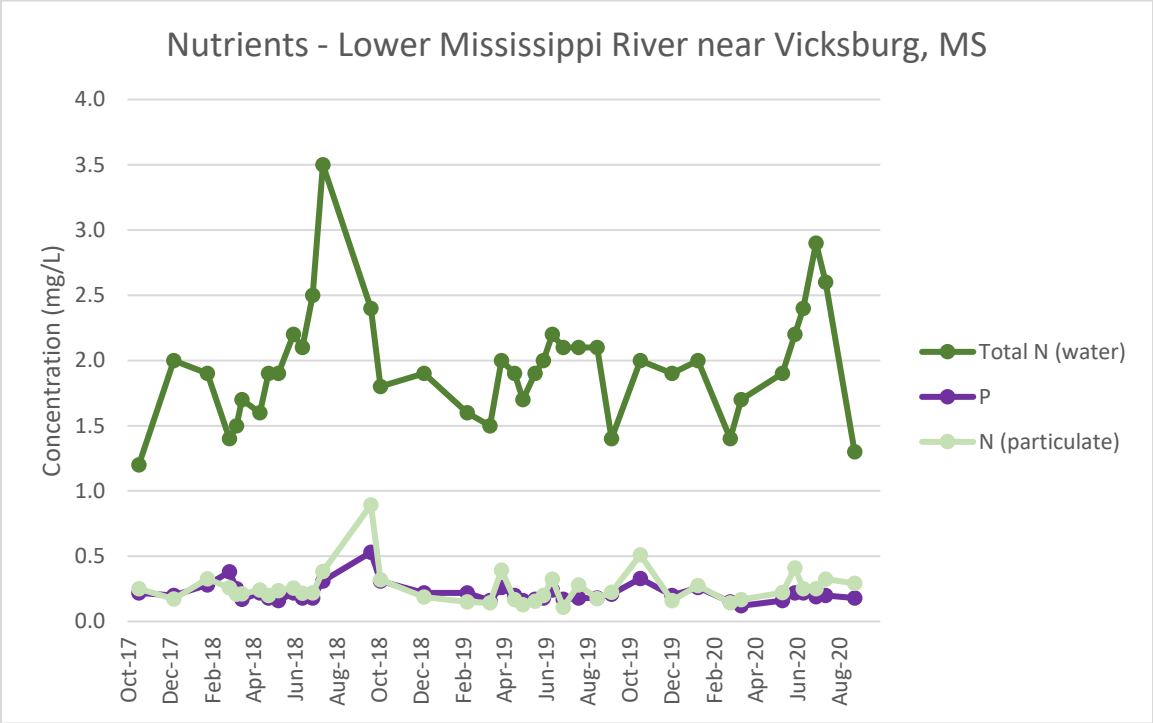

Figure 4.12 *Concentration of nutrients within the water column from the Vicksburg, MS water collection point. Data taken from USGS (accessed April 2022).*

CHAPTER V– DISCUSSION

5.1 Flood Comparison

5.1.1 Depositional Thickness & Grain Size

The observed differences in floodplain depositional thicknesses (fig. 4.1) are likely associated with flood durations; based on the premise that the longer a flood occurs within the floodplain, the more sediments can settle out of the water column. Greater depositional thicknesses in 2018- 19 are best explained by their combined flood durations; the 2019 flood being the longest in recorded history (fig. 4.7 & 4.8).

Where the 2019 flood is the longest in recorded history, it is not the largest flood recorded. In 2011, the LMR experienced the largest discharge event recorded. Sedimentation levels during this flood were less than those of the 2018-19 flood despite having more water influx on the floodplain. While there was more water, the flood duration was shorter resulting in lower depositional thicknesses in 2011 compared to 2018-19 (Heitmuller and others 2017). Differences in thickness can also be explained by flood water source. During the 2019 flood, between May and July, there was an increase in water being sourced from the Upper Mississippi, Arkansas, and Missouri rivers (fig. 4.8) whereas during the 2020 flood, most of the water was sourced from just the Ohio river (fig. 4.9).

Water-quality data from the USGS collected at Vicksburg, MS (station ID 322023090544500) upriver of our sample sites shows that during the 2018 flood, suspended sediment concentrations were at their highest and show the unusually early onset of the 2019 flood indicating an increase in available sediments for the floodplain with the short period of time between floods (fig. 4.10).

While flood duration is an important factor for depositional thickness, it is also crucial for the understanding of the grain size of the deposited sediments. Suspended sediment concentrations may also help explain the overall grain size distributions, more available silts and clays within the water column allow for increased deposition of finer grains (fig. 10). These data compounded with field and laboratory data indicates that the longer the flood water maintains a slower velocity compared to the main channel, the more fine-grained sediments are settled out of the water column and onto the floodplain.

Depositional thickness and grain size also vary depending on the geomorphic floodplain feature, for example, at the natural levee sample sites, the grain sizes were all >100 um (fig. 4.2) and the average thickness was ~ 250 mm (fig. 4.1) whereas at meander scrolls and backswamps, these values were considerably less. Overall comparison of all sediments collected between the 2018-19 flood and the 2020 flood shows that there is a significant difference in the grain sizes across all three environments sampled: natural levee, meander scroll, and backswamp (table 4.2).

Natural levees are elongated ridges that represent the boundary between the main river channel and the floodplain this leads to preferential deposition of sediments along the edge of the channel (Charlton 2008). When water crosses this boundary during times of flooding, there is a distinct decrease in velocity between the flow of the main channel and the floodplain flow (Charlton 2008). Larger grain sizes are quickly dropped from suspension and deposited at the time of this velocity decrease explaining why the larger grain sizes are found at the natural levee. Statistically, there is no mean difference in the grain size percentiles at natural levees between the 2018-19 samples and the 2020

samples (table 4.2) indicating that if samples were to be collected every year, the same grain size results would most likely be found at the natural levees.

Beyond the natural levees, remnant point bar deposits can occur (Charlton 2008). These deposits, called meander scrolls, create an undulating topography which consists of relative topographic highs (ridges) and relative topographic lows (swales) in arcuate patterns (Charlton 2008). This area of the floodplain consists mainly of finer grained, silt and clay sediments that were able to settle out of the water column during times of flooding (fig. 4.2). Statistically, when comparing the two floods at meander scroll locations, there is a mean difference in grain size for all values (table 4.2). Higher suspended sediment concentrations are the most reasonable explanation for this difference. During the rising limb of the 2018 flood, both the suspended sediment concentration and the sand percentage were relatively high which suggests that sand deposition may have been favored at the start of the 2018 flood (fig. 4.4). This high concentration of suspended sediments occurred again at the early rise in September 2018, but levels of silt and clay dominated the sediments during that period. The stages were moderate compared to the flood peaks in Winter/Spring 2018 & 2019. Therefore, this might have been a period of substantial fine-grained deposition in the floodplain due to high fine sediment concentrations and relatively shallow inundation in the floodplain. Finally, another good opportunity for sediment deposition in the floodplain especially sand (fig. 4.4) was early in the rising limb of the 2020 flood which explains the slightly higher D_{50} for 2020 deposits relative to the 2018-19 deposits (fig. 4.2).

Flood source is another reasonable explanation for this difference in grain sizes. In 2018-19, the flood waters were sourced from mainly the Ohio River with major

contributions from the Upper Mississippi, Missouri, and Arkansas rivers (fig. 4.8), which resulted in relatively high suspended sediment concentrations in the water column (fig. 4.10). In 2020 however, the flood was sourced mainly from the Ohio River (fig. 4.9) with lower levels of suspended sediments in the water column being transported to the meander scrolls (fig.4.4). Therefore, every year at meander scrolls, the sediments deposited would be different from the prior years collected samples.

Backswamps are the areas of the lowest elevation found on the floodplain typically behind a natural levee or distal from the main river channel (Charlton 2008). Overall deposition across the backswamp environment was less than the deposition at natural levee and meander scrolls (fig. 4.1). Sediments found within the backswamp were also finer grained silts and clays (fig. 4.2). These sites were often located farthest from the main river channel which explains why there was less sediment was deposited. Statistically, the backswamps show a mean difference within the finer grained samples (i.e., D_{10}, D_{16}, and D_{50}) with no mean difference for the coarser grains (D_{84}, D_{90}) (table 3.2). Being farthest from the main channel means that backswamps get the least amount of water during times of flooding which in turn decreases the amount of sediments deposited in this environment.

5.1.2 Organic Matter

Flood pulses provide valuable energy and material to the floodplain and as a result, floodplains decompose, produce, and export large volumes of OM which support the floodplain ecosystem (Noe and Hupp 2005). Values of OM may have been impacted by vegetation already found on the floodplain during the time of sampling. Higher levels of OM in 2018-19 indicate preservation favored by the extended duration of saturated

conditions or increased organic productivity in the warm overbank waters in the late summer of 2019. Levels of OM deposition indicates that there was more OM present after the 2020 flood than after the 2018-19 (fig. 3.3). Statistically, there is a mean difference in OM levels across all sediments collected (table 4.1).

Percent organics were lowest at natural levees with values of >1% measured for both years (fig. 4.3) caused by the high volume of sand being deposited at these sites rather than silts and clays (fig. 4.1). Organic matter particulates are most likely finer-grained than the sand and transported farther onto the floodplain via the water flow. These particulates are preserved for longer durations in fine-grained settings because oxygen and therefore microbial decomposition can be limited in these areas. High levels of OM measured at meander scrolls and backswamps where more silt and clay sized particles were deposited support this further transport of OM (fig. 4.2 & 4.3). Statistically, at natural levees and backswamps there is no mean difference between the two flood years (table 4.1). For the meander scrolls, there is a mean difference in OM across the two flood years (table 4.1). Meander scrolls are often the most vegetated region of the flood plain (Charlton 2008) so OM levels at these sites may have had plant material in the samples when collected. Backswamp OM levels for both years were relatively similar (fig. 4.3) and showed no mean difference statistically (table 4.1).

5.1.3 Carbon

Carbon (C) has two major sources into the environment, CO_2 in the atmosphere which dissolves in the hydrosphere to form $CaCO_3$ and C that enters the biosphere by photosynthesis (Faure 1991). A fraction of this biospheric C is deposited as organic matter (OM) in sediment and soil (Faure 1991). Carbon not related to organic

matter transported into the study area by floods is mostly from the decomposition of plants and animals on the floodplain. Total C levels for the 2020 flood were slightly higher than the 2018-19 flood samples, however, when divided into separate environments, only backswamp C values were higher in 2020 (fig. 3.4).

Natural levee sites had more carbon in 2018-19 than in 2020 and at meander scrolls, the levels were even for both years (fig. 4.4). Carbon, as well as OM are relatively low in sandy natural levee deposits than the fine-grained meander scrolls and backswamps. Since C levels are closely related to OM it is most likely due to the high levels of vegetation found at meander scrolls that led to these similar values each year. Statistically, this is also true, all sediments and all environments both had no mean difference in C values for 2018-19 and 2020 showing that these values will be similar after every flood (table 4.1). Carbon in the fluvial sediments near Vicksburg, MS, show that except for a few peaks in 2018, C concentrations remained relatively uniform indicating an even source of C to the floodplain (fig. 4.11). Concentrations of C indicate that post-flood organic activity rapidly converts available C to biological forms while diverse soil compositions and redox conditions equilibrate the remaining soil C to predictable levels commensurate with the floodplain setting (i.e., natural levees, meander scrolls, and backswamps).

5.1.4 Nutrients (nitrogen and phosphorus)

Floodplain soils are both a source and sink for vital nutrients such as nitrogen (N) and phosphorus (P) (Schramm and others 2009; Noe and Hupp 2005). Specifically, they can be sinks for organic, inorganic, dissolved, or particulate nitrogen and phosphorus

(Tockner and others 1999; Noe and Hupp 2005). Nutrients found in suspension near Vicksburg, MS, include particulate nitrogen, total nitrogen, and phosphorus (fig. 5.6).

Variation in overall nitrogen concentrations across all samples is indicative of a mean difference between the 2018-19 and 2020 flood sediments in terms of the nitrogen found at the three different environments (table 4.1). When narrowed down to nitrogen comparisons between the two flood years at the individual environments, there is no mean difference (table 4.1). This indicates that no matter where samples are collected at a natural levee, meander scroll or backswamp respectively, there will be little to no difference in nitrogen levels from year to year.

However, how this nitrogen came to be within the soil is important. Nitrogen is a highly dynamic element being found in both gas and solid forms. In normal non-saturated soils, nitrate and ammonium are high due to water drainage from the farmlands in the Midwest (Brown and others 2011). As a floodplain becomes more and more inundated, the soils become more anaerobic and saturated leading to denitrification (source). Although, when denitrification occurs, nitrogen becomes a gas and leaves the soil, high levels of nitrogen found in the water column at Vicksburg, may negate the effects of potential denitrification on the floodplain leaving relatively high levels of nitrogen in the soil (fig. 5.6).

Levels of nitrogen varied depending on floodplain environment (fig. 4.5). Natural levee sites for both years had the lowest total nitrogen content compared to meander scroll and backswamp sites (fig. 4.5). Lower levels of nitrogen found at natural levees is most likely related to the grain size and composition of the sediment, since at the natural levee sites, the sediment was mostly comprised of fine-grained sand (fig. 4.2). It is more

difficult for elements to adsorb themselves to sand sized particles compared to silts and clays (Weil and Brady textbook for soils). Furthermore, this explains why there is more nitrogen found at the meander scroll and backswamp sites (fig. 4.5). However, like C, N levels indicate that post- flood organic activity converts available N to biological forms while diverse soil compositions and redox conditions equalize the soil levels within floodplain environments.

Phosphorus levels within both the water column (fig. 5.6) and the floodplain soils were low with most sites having values of less than 0.1% (fig. 4.6). This is due to floodplain soils being a source of phosphorus to the water column during times of flooding (Schramm and others 2009). Like nitrogen, phosphorus is removed from soil as the conditions become anaerobic via the reduction and dissolution of phosphates, the release of clay- bound phosphates, and the hydrolysis and dissolution of iron and aluminum phosphates (Schramm and others 2009).

5.1.5 Magnetic Susceptibility

Magnetic susceptibility measures how much a material, in this case sediment, will become magnetized in a magnetic field. Measurements for both the 2018-19 samples and 2020 samples determined the sediments were both paramagnetic and diamagnetic for both years. This indicates that the source for both floods, while slightly different, had no real impact on the magnetic susceptibility of these sediments. Due to the paramagnetic and diamagnetic results, magnetic susceptibility results were not included in the statistical analyses and were taken at face value (appendix F).

5.2 Intrasite

Intrasite variation, variation within a site, across sites where four samples were collected show that there is limited variability across all samples. For intrasite ANOVA interactions, the environment is the most important factor. No variability at individual sites means that only one sample can be collected from each site and similar results would be achieved. Limited variability indicates that the conditions at each site were similar. While there is no mean difference in most of the interactions (table 4.3 & 4.4), the flood-comparison interactions for P, D84, and D90 don't follow that pattern. Differences in P can be explained by the measured zero values along sandy natural levees, as well as overall low levels of P at each site. Differences in larger grain sizes can be explained by differences in flood duration and overall suspended sediment concentrations.

5.3 Intersite

Intersite variation, variation across sites within the same environment, had limited variation for the year interaction indicating that there is a difference between sites between the two flood years. The only variable that had a mean difference was for the D_{90} grain size which is most likely due to differences in suspended sediment concentration and flood duration between 2018-19 and 2020. Majority of the variability determined by ANOVA was found for the environmental interaction (table 4.5 & 4.6). Variability amongst environments indicates that there are differences in flood conditions across the floodplain.

CHAPTER VI– CONCLUSIONS

The Lower Mississippi River (LMR) embanked floodplain near Natchez, MS experienced periods of inundation during the 2018, 2019, and 2020 water years, with the longest recorded flood occurring in 2019. Analysis of collected floodplain sediments from the 2018-19 flood deposits and 2020 flood deposits has led to a better understanding of the sedimentary characteristics and associated carbon and nutrient sequestration within this floodplain ecosystem. Overall comparison between the two floods shows there is a difference between depositional thickness, grain size, and carbon and nutrient levels in overbank sediments when comparing the 2018-19 and 2020 floods as well as differences comparing the different floodplain settings (natural levee, meander scroll, and backswamp). Local variability (intrasite) is limited between depositional thickness, grain size, carbon, and nutrient levels however, across floodplain settings, there is more variability, i.e., different sites within a meander scroll exhibit variation when compared to each other.

Offshore marine and coastal environments are explicitly impacted by upstream storage of sediment and nutrients which control shoreline positions and algal blooms that lead to anoxia respectively. Sedimentation of the floodplain greatly reduces the amount of sediment being transported to the coast of Louisiana. While there have been additional artificial controls along the main channels of the Missouri and Arkansas Rivers, land loss is still accelerated in Louisiana. If artificial controls are created to transport sediments downstream while maintaining nutrient influx to the floodplain via flood water, this land loss could be mitigated. Sustaining the sequestration of nutrients on the floodplain prevents the formation of harmful algal blooms in the Gulf of Mexico.

Sequestration that occurs on the LMR embanked floodplain is crucial to the ecosystem processes and nurture the diverse habitats of fish, waterfowl, plants, and other riparian species. Variability across the floodplain environments mean that nutrients are not equally distributed laterally. Should artificial controls be utilized on the LMR main channel, it is possible to transport nutrients to areas that are nutrient poor. Variation in nutrients in sediment plus the water data from the USGS indicates that most of the nutrients are transported and deposited by the flood water not the sediment, therefore the sediment can be theoretically separated from the nutrients and used to both maintain the alluvial floodplain ecosystem and mitigate coastal land loss in Louisiana.

Further research should be done on annual sedimentation and nutrient sequestration rates along the LMR embanked floodplain. Rates of sedimentation are dependent on a variety of factors including, flood duration and flood source. As more sediments are deposited on the floodplain, the available storage for water decreases causing the flood to spread laterally. Removal of sediment from the floodplain post flood, or the prevention of sediment deposition could benefit the coast of Louisiana. However, more information is needed on where the best places would be to either collect the sediment or where an artificial control structure would be most effective.

In terms of nutrient sequestration, more research needs to be done specifically on nutrient interactions on the floodplain and how they are deposited. Based on the data from the USGS compared relatively to the raw sediment data, most of the nutrients are transported onto the floodplain via the water. Limited amounts of the nutrients are left in the soil by the time sampling is conducted. Research on nutrient concentrations in the water column on the floodplain compared to within the main river channel would be

beneficial for understanding how to prevent nutrient dumping in the Gulf of Mexico further preventing anoxic zones caused by algal blooms. Higher levels of nutrients in the water column compared to the soils overall indicate that nutrient dumping can also be decreased by restoring natural floodplain environments along the LMR. Artificial controls are costly in both building and overall maintenance. With restored floodplain environments, levels of nitrogen and phosphorus in the water column would be further sequestered within the soils mitigating the effects of nutrient dumping in the Gulf of Mexico. While this project is a good start for understanding the overall sedimentation and sequestration processes that occur during times of flooding, there is always more to learn.

APPENDIX A – DEPOSITIONAL THICKNESSES

Table A.1 *Depositional thicknesses from the 2018-19 flood.*

Location	Thickness (mm)			
SCCNWR_055-19	28	32	26	
SANDSHEET_501-19	1430			
SCCNWR_056-19	108	100	105	
SCCNWR_057-19	85	87	68	
SCCNWR_502-19	140	145	167	
SCCNWR_503-19	70	62	65	
SCCNWR_058-19	49	58	65	
SCCNWR_059-19	59	57	55	
SCCNWR_504-19	56	54	50	
LOCHLEVEN_506-19	77	73	82	
LOCHLEVEN_505-19	51	48	33	
LOCHLEVEN_507-19	15	14	17	
LOCHLEVEN_508-19	12	14	18	
LOCHLEVEN_509-19	23	28	24	
LOCHLEVEN_510-19	54	64	58	
ARTONISH_01-01-00-19	280	265	280	
ARTONISH_01-002-10-19	234	230	225	236
ARTONISH_01-003-20-19	200	195	190	
ARTONISH_01-005-60-19	145	168	173	
ARTONISH_01-06-80-19	73	82	68	
ARTONISH_01-07-120-19	93	103	108	
CARTHAGEPT_040-19	21	24	22	
CLOVERDALEUnit_04-02-10-19	57	44	43	
CLOVERDALEUnit_04-03-20-19	44	44	51	
CLOVERDALEUnit_04-04-40-19	31	33	33	
CLOVERDALEUnit_04-05-50-19	29	26	29	
CLOVERDALEUnit_04-06-61-19	29	31	31	
CLOVERDALEUnit_04-07-80-19	29	25	28	
CLOVERDALEUnit_04-08-90-19	28	24	24	
CLOVERDALEUnit_04-09-100-19	28	24	36	25
CLOVERDALEUnit_04-10-110-19	24	36	18	28
CLOVERDALEUnit_04-11-120-19	29	29	36	

Table A.1 (continued).

CLOVERDALEUnit_04-12-130-19	37	38	29	34
CLOVERDALEUnit_Pad036-19	28	24	26	
CLOVERDALEUnit_05-01-00B	30	34	38	
CLOVERDALEUnit_05-02-10-19	36	42	40	
CLOVERDALEUnit_05-03-20-19	33	28	31	
CLOVERDALEUnit_511-19	19	24	24	
CARTHAGEPT_512-19	750			
BUTLERLAKE_07-01-19	36	32	26	
BUTLERLAKE_07-02-19	24	27	16	
SALTLAKE_08-01-19	31	28	26	
SALTLAKE_08-02-19	17	18	20	
SALTLAKE_08-03-19	18	19	21	
SALTLAKE_08-04-19	10	12	15	
SALTLAKE_08-05-19	13	21	18	
SIBLEYUNIT_513-19	24	27	21	18
SIBLEYUNIT_514-19	48	40	44	

Table A.2 *Depositional thicknesses from the 2020 flood.*

Location	Thickness (mm)			
SCCNWR_503-20	8	7	6	
SCCNWR_058-20	6	8	11	
SCCNWR_059-20	9	9	10	
SCCNWR_504-20	6	7	6	
LOCHLEVEN_506-20	38	21	33	
LOCHLEVEN_505-20	5	6	4	
LOCHLEVEN_507-20	10	3	10	
LOCHLEVEN_508-20	3	4	3	
LOCHLEVEN_509-20	5	4	8	
LOCHLEVEN_510-20	10	8	9	
ARTONISH_01-01-00-20	100	110	120	
ARTONISH_01-002-10-20	165	170	150	
ARTONISH_01-003-20-20	70	40	50	
ARTONISH_01-005-60-20	120	120	115	
ARTONISH_01-06-80-20	75	50	55	
ARTONISH_01-07-120-20	11	10	10	

Table A.2 (continued).

CARTHAGEPT_040-20	0	0	0	0
CLOVERDALEUnit_04-02-10-20	5	6	6	
CLOVERDALEUnit_04-03-20-20	12	18	14	
CLOVERDALEUnit_04-04-40-20	11	18	16	
CLOVERDALEUnit_04-05-50-20	14	16	17	
CLOVERDALEUnit_04-06-61-20	9	13	12	
CLOVERDALEUnit_04-07-80-20	14	11	18	
CLOVERDALEUnit_04-08-90-20	15	18	16	
CLOVERDALEUnit_04-09-100-20	22	15	10	
CLOVERDALEUnit_04-10-110-20	12	8	8	
CLOVERDALEUnit_04-11-120-20	15	10	8	
CLOVERDALEUnit_04-12-130-20	9	5	15	
CLOVERDALEUnit_Pad36-20	14	13	14	
CLOVERDALEUnit_05-01-00B-20	14	18	12	
CLOVERDALEUnit_05-02-10-20	10	6	9	
CLOVERDALEUnit_05-03-20-20	6	8	7	
CLOVERDALEUnit_511-20	7	8	8	
CARTHAGEPT_512-20	0	0	0	0
BUTLERLAKE_07-01-20	10	6	8	
BUTLERLAKE_07-02-20	11	12	11	
SALTLAKE_08-01-20	70	73	70	
SALTLAKE_08-02-20	55	70	70	
SALTLAKE_08-03-20	3	4	4	
SALTLAKE_08-04-20	6	6	5	
SALTLAKE_08-05-20	5	9	8	
SIBLEYUNIT_513-20	10	15	19	
SIBLEYUNIT_514-20	10	12	10	

APPENDIX B –RAW CARBON AND NITROGEN WEIGHT PERCENTS

Table B.1 *Raw weight percent of carbon and nitrogen from the 2018-19 flood sediments.*

Site ID	Wt % Nitrogen	Wt % Carbon
SCCNWR_055-19	0.01	0.20
	0.02	0.22
	0.01	0.15
	0.01	0.21
SandSht_501-19	0.02	0.19
SCCNWR_056-19	0.07	1.08
	0.09	1.39
	0.08	1.22
	0.08	1.27
SCCNWR_057-19	0.16	1.92
	0.12	1.58
	0.15	1.79
	0.14	1.70
SCCNWR_502-19	0.16	2.02
	0.18	2.51
	0.15	1.79
	0.16	1.89
SCCNWR_503-19	0.17	1.96
	0.19	2.16
	0.18	1.98
	0.19	2.10
SCCNWR_058-19	0.29	3.21
	0.22	2.50
	0.28	3.17
	0.22	2.53
SCCNWR_059-19	0.26	3.18
	0.28	3.38
	0.17	2.15
	0.27	3.36
SCCNWR_504-19	0.17	2.08
	0.27	3.54
	0.17	2.10
	0.18	2.29
LOCHLEVEN_506-19	0.18	2.03
	0.19	2.24
	0.19	2.11
	0.17	2.03

Table B.1 (continued).

LOCHLEVEN_505-19	0.14	1.85
	0.13	1.61
	0.13	1.64
	0.15	1.83
LOCHLEVEN_507-19	0.25	3.25
	0.37	4.70
	0.30	3.78
	0.38	5.20
LOCHLEVEN_508-19	0.25	2.89
	0.27	3.14
	0.29	3.46
	0.28	3.43
LOCHLEVEN_509-19	0.28	3.14
	0.22	2.63
	0.25	2.86
	0.27	3.08
LOCHLEVEN_510-19	0.21	2.37
	0.21	2.49
	0.23	2.81
	0.22	2.58
ARTONISH_01-01-00-19	0.01	0.16
	0.02	0.58
	0.01	0.18
	0.01	0.13
ARTONISH_01-002-10-19	0.01	0.32
	0.00	0.12
ARTONISH_01-003-20-19	0.02	0.31
ARTONISH_01-005-60-19	0.00	0.23
ARTONISH_01-06-80-19	0.01	0.14
ARTONISH_01-07-120-19	0.11	2.06
	0.04	1.11
	0.04	0.80
	0.06	1.10
CARTHAGEPT_040-19	0.01	0.30
CLOVERDALEUnit_04-02-10-19_Pad25	0.29	3.06
	0.27	2.81
	0.27	2.71
	0.39	3.77
CLOVERDALEUnit_04-03-20-19_Pad26	0.25	2.55
CLOVERDALEUnit_04-04-40-19_Pad27	0.28	2.79

Table B.1 (continued).

CLOVERDALEUnit_04-05-50-19_Pad28	0.31	3.21
CLOVERDALEUnit_04-06-61-19_Pad29	0.30	2.97
	0.27	2.93
	0.29	3.05
	0.27	3.02
CLOVERDALEUnit_04-07-80-19_Pad30	0.34	3.45
CLOVERDALEUnit_04-08-90-19_Pad31	0.33	3.27
CLOVERDALEUnit_04-09-100-19_Pd32	0.27	2.87
CLOVERDALEUnit_04-10-110-19_Pd33	0.28	3.02
CLOVERDALEUnit_04-11-120-19_Pd34	0.26	2.90
	0.29	3.29
	0.32	3.46
	0.31	3.60
CLOVERDALEUnit_04-12-130-19_Pd35	0.28	3.16
CLOVERDALEUnit_Pad036-19	0.22	2.49
CLOVERDALEUnit_05-01-00B_PD37	0.24	2.57
	0.27	3.03
	0.27	3.12
	0.28	2.95
CLOVERDALEUnit_05-02-10-19_Pd38	0.22	2.51
CLOVERDALEUnit_05-03-20-19_Pd39	0.23	2.67
CLOVERDALEUnit_511-19	0.23	2.85
	0.24	3.04
	0.23	2.99
	0.25	3.51
CARTHAGEPT_512-19	0.01	0.14
BUTLERLAKE_07-01-19_Pad41	0.24	2.63
	0.37	4.30
	0.43	5.22
	0.52	5.74
BUTLERLAKE_07-02-19_Pad042	0.23	2.37
SALTLAKE_08-01-19_Pad43	0.34	4.43
	0.41	6.00
	0.45	5.91
	0.36	4.84
SALTLAKE_08-02-19_Pad044	0.32	3.98
SALTLAKE_08-03-19_Pad045	0.34	4.52

Table B.1 (continued).

SALTLAKE_08-04-19_Pad046	0.35	4.45
	0.32	4.25
	0.37	4.84
	0.30	3.72
SALTLAKE_08-05-19_Pad047	0.34	4.26
SIBLEYUNIT_513-19	0.17	2.30
SIBLEYUNIT_514-19	0.15	2.11

Table B.2 *Raw weight percent of carbon and nitrogen from the 2020 flood sediments.*

Site ID	Wt. % Nitrogen	Wt. % Carbon
SCCNWR_503-20	0.27	3.19
	0.27	3.24
	0.32	3.83
	0.25	2.85
SCCNWR_058-20	0.23	2.51
	0.33	3.72
	0.25	2.83
	0.27	2.83
SCCNWR_059-20	0.28	3.24
	0.3	3.37
	0.29	3.28
	0.26	3.08
SCCNWR_504-20	0.18	2.16
	0.15	1.92
	0.18	2.13
	0.19	2.18
LOCHLEVEN_506-20	0.28	4.53
	0.32	5.02
	0.3	4.33
	0.24	3.34
LOCHLEVEN_505-21	0.17	1.95
	0.15	1.71
	0.16	1.83
	0.21	2.62

Table B.2 (continued).

LOCHLEVEN_507-22	0.41	5.09
	0.34	4.39
	0.37	4.94
	0.49	6.71
LOCHLEVEN_508-23	0.43	5.4
	0.36	4.36
	0.4	4.82
	0.37	4.5
LOCHLEVEN_509-24	0.25	2.85
	0.23	2.36
	0.24	2.73
	0.27	2.9
LOCHLEVEN_510-25	0.3	3.13
	0.27	2.79
	0.26	2.83
	0.25	2.72
ARTONISH_01-01-00-20	0.01	0.17
	0.01	0.2
	0.01	0.22
	0.02	0.24
ARTONISH_01-002-10-20	0.02	0.44
ARTONISH_01-003-20-20	0.04	0.64
ARTONISH_01-005-60-20	0.02	0.42
ARTONISH_01-06-80-20	0.01	0.31
ARTONISH_01-07-120-20	0.07	1.13
CARTHAGEPT_040-20	0.01	0.26
CLOVERDALE_04-02-10-20	0.31	3.28
	0.3	3.2
	0.34	3.62
	0.25	2.88
CLOVERDALE_04-03-20-20	0.27	3.04
CLOVERDALE_04-04-40-20	0.36	3.67
CLOVERDALE_04-05-50-20	0.33	3.36

Table B.2 (continued)

CLOVERDALE_04-06-61-20	0.33	3.51
	0.32	3.66
	0.31	3.33
	0.33	3.39
CLOVERDALE_04-07-80-20	0.32	3.26
CLOVERDALE_04-08-90-20	0.33	3.43
CLOVERDALE_04-09-100-20	0.3	3.24
CLOVERDALE_04-10-110-20	0.31	3.43
CLOVERDALE_04-11-120-20	0.25	2.78
	0.26	3.01
	0.25	2.79
	0.27	3.06
CLOVERDALE_04-12-130-20	0.29	3.29
CLOVERDALE_PAD036	0.25	2.71
CLOVERDALE_05-01-00B	0.22	2.48
	0.21	2.47
	0.24	2.66
	0.21	2.39
CLOVERDALE_05-02-10-20	0.2	2.28
CLOVERDALE_05-03-20-20	0.21	2.61
CLOVERDALE_511-20	0.19	2.68
	0.21	3.21
	0.18	2.53
	0.17	2.13
CARTHAGE PT_512-20	0.03	0.32
BUTLER LAKE_07-01-20	0.22	2.74
	0.25	3.09
	0.22	2.55
	0.23	2.79
BUTLER LAKE_07-02-20	0.2	2.34
SALT LAKE_08-01-20	0.24	3.78
	0.25	3.64
	0.26	4.43
	0.25	6.37
SALT LAKE_08-02-20	0.2	3.07
SALT LAKE_08-03-20	0.2	2.86

Table B.2 (continued).

SALT LAKE_08-04-20	0.2	2.62
	0.2	2.59
	0.21	2.78
	0.21	2.85
SALT LAKE_08-05-20	0.21	2.78
SIBLEY_513-20	0.09	1.44
SIBLEY_514-20	0.12	1.75

APPENDIX C – RAW ORGANIC MATTER PERCENTAGES

Table C.1 *Percent organics from the 2018-19 flood sediments*

Site ID	Percent Organics
SCCNWR_055-19	0.125649811
	0.181244542
	0.134795246
	0.124494291
SANDSHEET_501-19	0.110268141
SCCNWR_056-19	0.769048101
	0.791643636
	0.854824932
	1.071704324
SCCNWR_057-19	1.446453799
	1.403723117
	1.394214556
	1.12654122
SCCNWR_502-19	1.569912567
	1.668693159
	1.416587955
	1.962024523
SCCNWR_503-19	2.237940064
	2.443760313
	2.265863352
	2.085206835
SCCNWR_058-19	2.473992905
	2.333260822
	1.994253895
	2.015694332
SCCNWR_059-19	1.390036933
	1.520429538
	1.771440943
	1.804869402
SCCNWR_504-19	1.395186272
	1.916637794
	1.672240803
	1.463149733

Table C.1 (continued).

LOCHLEVEN_506-19	1.847160561
	2.01909032
	1.773045342
	1.564320233
LOCHLEVEN_505-19	1.569987855
	1.479857447
	1.939278587
	1.503592539
LOCHLEVEN_507-19	2.2044519
	2.658167067
	2.885765161
	3.580500448
LOCHLEVEN_508-19	2.808047189
	2.73465881
	3.257076822
	3.395863061
LOCHLEVEN_509-19	2.855434003
	1.751539334
	1.544185016
	1.933175153
LOCHLEVEN_510-19	1.90027358
	1.991080415
	2.029880033
	2.065005731
ARTONISH_01-01-00-19	0.11846305
	0.232209507
	0.168576303
	0.173496133
ARTONISH _01-002-10-19	0.249901939
	0.116443026
ARTONISH _01-003-20-19	0.339529328
ARTONISH _01-005-60-19	0.165470025
ARTONISH _01-06-80-19	0.193215363

Table C.1 (continued).

ARTONISH _01-07-120-19	0.810201297
	0.851001384
	0.758152381
	1.094919189
CARTHAGE PT_040-19	0.234971824
CLOVERDALE_04-02-10-19	2.706213562
	2.408645166
	2.142273607
	2.416655582
CLOVERDALE _04-03-20-19	1.79514643
CLOVERDALE_04-04-40-19	1.811055103
CLOVERDALE _04-05-50-19	1.903017571
CLOVERDALE _04-06-61-19	2.037992936
	1.91819327
	2.576665646
	2.481928095
CLOVERDALE _04-07-80-19	2.059265931
CLOVERDALE _04-08-90-19	2.038260309
CLOVERDALE _04-09-100-19	2.71666282
CLOVERDALE _04-10-110-19	2.180321127
CLOVERDALE_04-11-120-19	2.890483839
	2.317540061
	2.633218274
	2.428463264
CLOVERDALE _04-12-130-19	2.523531715
CLOVERDALE _PAD036	2.505982761

Table C.1 (continued).

CLOVERDALE _05-01-00B	2.446937925
	1.333689532
	2.211708275
	2.447029965
CLOVERDALE _05-02-10-19	2.109894526
CLOVERDALE _05-03-20-19	2.606548364
CLOVERDALE _511-19	2.120264861
	2.567251189
	2.197986618
	2.42937833
CARTHAGE PT_512-19	0.124713643
BUTLER LAKE_07-01-19	2.417090952
	2.538501363
	3.044467939
	3.128184179
BUTLER LAKE_07-02-19	2.289054638
SALT LAKE_08-01-19	3.790704202
	3.632765238
	4.383768975
	4.30764286
SALT LAKE _08-02-19	3.202862894
SALT LAKE _08-03-19	3.718226988
SALT LAKE_08-04-19	4.123698695
	3.331531291
	3.58528506
	3.519640279
SALTLAKE_08-05-19	3.872453769
SIBLEY_513-19	1.865444682
SIBLEY _514-19	1.674714909

Table C.2 *Percent organics from the 2020 flood sediments.*

Site	percent organics
SCCNWR_503-20	3.325677224
	2.452573492
	2.470326537
	1.979328981
SCCNWR_058-20	1.732455411
	2.753693277
	2.033721371
	2.683872854
SCCNWR_059-20	2.22041778
	2.813483947
	2.840925446
	3.080107364
SCCNWR_504-20	1.75396188
	1.70766847
	1.634704251
	1.753354595
LOCHLEVEN_506-20	2.042848412
	2.383164954
	2.12602326
	2.434296818
LOCHLEVEN_505-21	1.540062638
	1.321607044
	1.68743318
	1.637313134
LOCHLEVEN_507-22	2.538220913
	2.017771568
	2.704170301
	2.324442015
LOCHLEVEN_508-23	2.541072902
	2.324139368
	2.144146569
	2.223010345

Table C.2 (continued).

LOCHLEVEN_509-24	1.774452709
	2.237729906
	2.023691802
	1.983958488
LOCHLEVEN_510-25	2.241700105
	1.669040668
	2.658785961
	2.211240581
ARTONISH_01-01-00-20	0.188368792
	0.153314486
	0.216593623
	0.23656763
ARTONISH_01-002-10-20	0.25705152
ARTONISH_01-003-20-20	0.786123831
ARTONISH_01-005-60-20	0.165826233
ARTONISH_01-06-80-20	0.228029183
ARTONISH_01-07-120-20	0.834292414
CARTHAGEPT_040-20	0.201365302
CLOVERDALE_04-02-10-20	2.872769885
	1.885921107
	2.536839707
	2.630335103
CLOVERDALE_04-03-20-20	2.072888469
CLOVERDALE_04-04-40-20	1.819347053
CLOVERDALE_04-05-50-20	1.80276716
CLOVERDALE_04-06-61-20	1.927759106
	1.820750473
	3.208666756
	2.17232066
CLOVERDALE_04-07-80-20	2.374043894
CLOVERDALE_04-08-90-20	2.348926911
CLOVERDALE_04-09-100-20	1.850095448
CLOVERDALE_04-10-110-20	2.138702206

Table C.2 (continued).

CLOVERDALE_04-11-120-20	2.148182649
	2.150052228
	2.276726591
	2.551827077
CLOVERDALE_04-12-130-20	1.842698709
CLOVERDALE_PAD036	1.883426178
CLOVERDALE_05-01-00B	1.494156265
	2.100920759
	2.027583986
	1.932519445
CLOVERDALE_05-02-10-20	1.947006579
CLOVERDALE_05-03-20-20	2.322416287
CLOVERDALE_511-20	1.817883209
	2.301662152
	1.796736836
	1.89961226
CARTHAGE PT_512-20	0.269636057
BUTLER LAKE_07-01-20	2.131486563
	2.654682517
	2.600999128
	2.441761109
BUTLER LAKE_07-02-20	2.376350762
SALT LAKE_08-01-20	2.775629309
	2.327724613
	2.891754302
	3.050815824
SALT LAKE_08-02-20	2.289525272
SALT LAKE_08-03-20	3.956245474
SALT LAKE_08-04-20	1.769128672
	2.158481524
	2.805396803
	2.51293754
SALT LAKE_08-05-23	2.357269872
SIBLEY_513-20	1.27676496
SIBLEY_514-20	1.370849802

APPENDIX D – RAW PHOSPHORUS WEIGHT PERCENTS

Table D.1 *Raw weight percent phosphorus for the 2018-19 flood sediments.*

Site	Sample
	Phosphorus (%)
SCCNWR_055-19	0.0341
	0.0340
	0.0308
	0.0393
SANDSHEET_501-19	0.0345
SCCNWR_056-19	0.0560
	0.0750
	0.0685
	0.0654
SCCNWR_057-19	0.1018
	0.0714
	0.0764
	0.0884
SCCNWR_502-19	0.0837
	0.0803
	0.0731
	0.0819
SCCNWR_503-19	0.0905
	0.0855
	0.0801
	0.0879
SCCNWR_058-19	0.1003
	0.1120
	0.1012
	0.0942
SCCNWR_059-19	0.0839
	0.1034
	0.0847
	0.0910
SCCNWR_504-19	0.0763
	0.0895
	0.0869
	0.0816
LOCHLEVEN_506-19	0.0967
	0.0797
	0.0949
	0.0841

Table D.1 (continued).

LOCHLEVEN_505-19	0.0777
	0.0671

	0.0731
	0.0639
LOCHLEVEN_507-19	0.0921
	0.0920
	0.0742
	0.0651
LOCHLEVEN_508-19	0.0827
	0.0895
	0.0810
	0.0862
LOCHLEVEN_509-19	0.1063
	0.0789
	0.0846
	0.0937
LOCHLEVEN_510-19	0.0855
	0.0742
	0.0885
	0.0799
ARTONISH_01-01-00-19	0.0073
	0.0115
	0.0267
	0.0504
ARTONISH_01-002-10-19	0.0407
	0.0284
ARTONISH_01-003-20-19	0.0302
ARTONISH_01-005-60-19	0.0334
ARTONISH_01-06-80-19	0.0330
ARTONISH_01-07-120-19	0.0269
	0.0293
	0.0172
	0.0273
CARTHAGEPT_040-19	0.0394
CLOVERDALEUnit_04-02-10-19	0.0918
	0.0847
	0.1195
	0.1014
CLOVERDALEUnit_04-03-20-19	0.0927
CLOVERDALEUnit_04-04-40-19	0.1241

Table D.1 (continued).

CLOVERDALEUnit_04-05-50-19	0.0974

CLOVERDALEUnit_04-06-61-19	0.0781
	0.0826
	0.0853
	0.1119
CLOVERDALEUnit_04-07-80-19	0.1001
CLOVERDALEUnit_04-08-90-19	0.1005
CLOVERDALEUnit_04-09-100-19	0.0851
CLOVERDALEUnit_04-10-110-19	0.0789
CLOVERDALEUnit_04-11-120-19	0.1137
	0.0744
	0.0909
	0.0864
CLOVERDALEUnit_04-12-130-19	0.0960
CLOVERDALEUnit_Pad036-19	0.1167
CLOVERDALEUnit_05-01-00B-19	0.0623
	0.0581
	0.0684
	0.0734
CLOVERDALEUnit_05-02-10-19	0.0668
CLOVERDALEUnit_05-03-20-19	0.0702
CLOVERDALEUnit_511-19	0.0711
	0.0649
	0.0677
	0.0775
CARTHAGEPT_512-19	0.0071
BUTLERLAKE_07-01-19	0.0893
	0.1164
	0.0790
	0.1028
BUTLERLAKE_07-02-19	0.0970
SALTLAKE_08-01-19	0.1042
	0.1121
	0.1026
	0.1162
SALTLAKE_08-02-19	0.1123
SALTLAKE_08-03-19	0.0859
SALTLAKE_08-04-19	0.0851
	0.0983
	0.0807
	0.0926

Table D.1 (continued)

SALTLAKE_08-05-19	0.0743

SIBLEYUNIT_513-19	0.0479
SIBLEYUNIT_514-19	0.0458

Table D.2 *Raw weight percent phosphorus for the 2020 flood sediments.*

Site	Sample Phosphorus (%)
SCCNWR_503-20	0.0971
	0.0776
	0.0786
	0.0818
SCCNWR_058-20	0.0974
	0.0924
	0.0934
	0.0645
SCCNWR_059-20	0.0769
	0.0597
	0.0679
	0.0600
SCCNWR_504-20	0.0410
	0.0340
	0.0280
	0.0330
LOCHLEVEN_506-20	0.0440
	0.1110
	0.0493
	0.0570
LOCHLEVEN_505-21	0.0522
	0.0568
	0.0486
	0.0528
LOCHLEVEN_507-22	0.0724
	0.0948
	0.0660
	0.0897
LOCHLEVEN_508-23	0.0674
	0.0692
	0.0655
	0.0588

Table D.2 (continued).

LOCHLEVEN_509-24	0.0740
	0.0560
	0.0596
	0.0530
LOCHLEVEN_510-25	0.0557
	0.0837
	0.0551
	0.0722
ARTONISH_01-01-00-20	0.0000
	0.0000
	0.0000
	0.0000
ARTONISH_01-002-10-20	0.0053
ARTONISH_01-003-20-20	0.0000
ARTONISH_01-005-60-20	0.0073
ARTONISH_01-06-80-20	0.0070
ARTONISH_01-07-120-20	0.0176
CARTHAGEPT_040-20	0.0165
CLOVERDALE_04-02-10-20	0.0979
	0.0895
	0.2298
	0.0831
CLOVERDALE_04-03-20-20	0.0957
CLOVERDALE_04-04-40-20	0.0899
CLOVERDALE_04-05-50-20	0.1004
CLOVERDALE_04-06-61-20	0.0803
	0.0841
	0.0620
	0.1017
CLOVERDALE_04-07-80-20	0.0901
CLOVERDALE_04-08-90-20	0.0821
CLOVERDALE_04-09-100-20	0.0700
CLOVERDALE_04-10-110-20	0.0703
CLOVERDALE_04-11-120-20	0.0614
	0.0846
	0.0864
	0.0863
CLOVERDALE_04-12-130-20	0.0743
CLOVERDALE_PAD036	0.0642

Table D.2 (continued).

CLOVERDALE_05-01-00B	0.0855
	0.0467

	0.1004
	0.0724
CLOVERDALE_05-02-10-20	0.0861
CLOVERDALE_05-03-20-20	0.0656
CLOVERDALE_511-20	0.0410
	0.0514
	0.1060
	0.1071
CARTHAGE PT_512-20	0.1038
BUTLER LAKE_07-01-20	0.2082
	0.2090
	0.1925
	0.1641
BUTLER LAKE_07-02-20	0.1457
SALT LAKE_08-01-20	0.1489
	0.1180
	0.1146
	0.0972
SALT LAKE_08-02-20	0.1163
SALT LAKE_08-03-20	0.1080
SALT LAKE_08-04-20	0.1033
	0.1252
	0.1438
	0.1820
SALT LAKE_08-05-23	0.1088
SIBLEY_513-20	0.0830
SIBLEY_514-20	0.0505

APPENDIX E – RAW GRAIN SIZE VALUES

Table E.1 *Raw grain size values for the 2018-19 flood sediments.*

Site ID	D_{10}	D_{16}	D_{50}	D_{84}	D_{90}
SCCNWR_055-19	77.78452	95.91669	155.1318	228.3273	250.7729
	67.94607	80.47192	114.6529	156.3829	168.8037
	117.5678	128.7347	179.1539	244.7433	264.2035
	113.0106	129.4599	206.9373	313.046	347.0912
SANDSHEET_501-19	115.6923	128.2219	186.3814	266.2359	291.1806
SCCNWR_056-19	3.112306	5.759723	43.22914	311.1683	372.1172
	2.941871	5.585501	39.42324	166.8042	225.8594
	5.526321	11.63085	112.7314	187.8744	209.1518
	1.607187	3.377535	20.86306	43.56579	49.33192
SCCNWR_057-19	1.081687	2.574454	10.07376	28.94064	35.27106
	1.036119	2.395688	9.718536	27.05068	32.64173
	0.784627	1.663454	8.291978	26.13926	32.96405
	0.618383	0.922732	7.781148	28.04526	33.9928
SCCNWR_502-19	0.781261	1.625296	7.512747	23.7145	30.67086
	1.121108	2.599958	10.58867	32.35878	39.84897
	0.960395	2.197458	10.34378	34.43468	46.09852
	0.856383	1.9695	8.974185	27.08908	33.22478
SCCNWR_503-19	0.836404	1.791608	8.031441	23.77633	29.66352
	0.905100	1.933921	8.299487	26.77728	33.68481
	0.896019	2.053975	8.538537	27.44123	36.98973
	0.829962	1.789207	7.896984	25.42796	33.94524
SCCNWR_058-19	0.881191	2.105391	9.214288	29.96439	40.62274
	0.728302	1.390125	7.243619	22.46005	29.47925
	0.74724	1.594415	8.970174	65.57767	105.3442
	0.811603	1.786356	7.763766	23.85956	31.29576
SCCNWR_059-19	0.798705	1.681614	7.861002	24.65481	32.65094
	0.95431	2.262763	9.070227	29.15357	38.72057
	0.821617	1.746704	8.384662	21.54373	25.60665
	0.723898	1.427621	7.726104	24.74306	32.19585
SCCNWR_504-19	1.010516	2.475544	11.452	30.21193	35.76078
	0.892735	2.063095	10.93855	33.56679	42.93274
	1.427542	3.125756	13.78284	33.98551	39.61411
	0.993681	2.371291	10.12244	29.22368	35.86590
LOCHLEVEN_506-19	0.517236	0.77193	5.313022	15.18655	19.25949
	0.639466	0.911235	5.059467	12.26779	15.15682
	0.413405	0.67827	4.818449	14.21429	18.67254
	0.786807	1.671442	8.062167	20.17757	25.39387

Table E.1 (continued).

LOCHLEVEN_505-19	0.657127	1.107896	7.304787	21.61602	26.6559
	0.7689	1.702	6.816	19.19	25.48
	2.25	3.794	13.52	37.52	48.54
	0.799579	1.784533	8.664497	23.40488	28.16227
LOCHLEVEN_507-19	0.581001	0.839124	5.584019	15.3247	20.4867
	0.661044	1.040816	6.442713	18.95661	25.77948
	0.658731	1.068271	6.142479	16.17841	20.12419
	0.71227	1.211267	6.445908	16.41423	20.71933
LOCHLEVEN_508-19	0.627263	0.91631	5.356379	12.73702	15.36737
	0.546856	0.784467	4.919726	12.07511	14.9655
	0.616015	1.015565	5.8695	14.91538	18.80729
	0.622101	0.934021	5.205334	12.96449	16.32855
LOCHLEVEN_509-19	0.82988	1.79923	7.671056	21.62612	27.33976
	0.73836	1.367037	6.152359	14.84535	18.52055
	0.74975	1.392917	6.343032	15.81336	19.60311
	0.593909	0.888053	5.562666	14.83953	18.92551
LOCHLEVEN_510-19	0.604482	0.92346	5.491981	14.2788	18.08633
	0.560425	0.882334	5.932922	16.68397	21.55371
	0.590634	0.856719	5.611714	16.19414	21.80743
	0.418787	0.571141	4.194055	12.17356	15.99404
ARTONISH_01-01-00-19	113.3382	126.2204	185.2688	265.2043	290.5402
	121.4637	135.1021	198.7402	283.911	309.2816
	124.7866	137.7933	200.062	283.3727	308.0001
	128.1921	141.5384	203.4449	286.0686	310.2343
ARTONISH _01-002-10-19	74.78467	90.47136	149.2632	225.5783	249.3472
	146.215	160.4052	225.8278	311.6403	338.9739
ARTONISH _01-003-20-19	73.8107	109.4589	188.612	280.1136	307.9367
ARTONISH _01-005-60-19	111.5133	122.8937	177.5083	251.1644	273.1162
ARTONISH _01-06-80-19	112.7716	124.2086	177.8975	250.2573	271.4355
ARTONISH _01-07-120-19	4.870689	9.81389	77.80028	141.8996	160.4364
	15.20024	46.05702	106.8907	166.231	184.5895
	7.817569	17.76326	94.65365	160.3538	180.0905
	3.874769	7.201582	58.46913	146.7692	174.0143
CARTHAGE PT_040-19	84.37356	97.87642	153.5524	227.1896	249.9067
CLOVERDALE_04-02-10-19	0.681463	1.138119	5.696621	14.95509	19.43094
	0.559669	0.862998	5.49221	14.4348	18.47185
	0.530529	0.841537	5.078348	12.99085	16.6608
	0.586523	0.890351	5.394482	13.83701	17.52916
CLOVERDALE _04-03-20-19	0.657594	1.12001	5.802405	14.2538	17.82944
CLOVERDALE_04-04-40-19	0.550714	0.916516	4.799421	11.31734	14.21536
CLOVERDALE _04-05-50-19	0.764189	1.534776	6.211107	16.40604	22.00413

Table E.1 (continued).

CLOVERDALE _04-06-61-19	0.61032	0.915089	5.495341	13.98746	17.42112
	0.573422	0.845533	5.079882	12.33263	15.16997
	0.716753	1.347629	5.900212	15.05909	19.14152
	0.508046	0.758806	5.132149	12.99207	16.46161
CLOVERDALE _04-07-80-19	0.662636	1.168142	6.920579	21.56231	30.40562
CLOVERDALE _04-08-90-19	0.516898	0.786069	6.335635	22.95555	35.74001
CLOVERDALE _04-09-100-19	0.751051	1.400302	5.755835	13.9689	17.37748
CLOVERDALE _04-10-110-19	0.525815	0.825763	5.186143	13.0338	16.7066
CLOVERDALE_04-11-120-19	0.54009	0.84946	5.546745	14.54279	18.80636
	0.613192	0.952347	5.573876	14.49316	18.82552
	0.494332	0.752136	5.576657	16.28582	22.23308
	0.639956	1.065836	5.726209	15.02805	19.71042
CLOVERDALE _04-12-130-19	0.416763	0.642906	5.022497	13.50986	17.54606
CLOVERDALE _PAD036	0.492186	0.786982	5.397594	14.34593	18.21599
CLOVERDALE _05-01-00B	0.025412	0.034711	0.353682	9.40996	14.35781
	0.026058	0.036231	0.852079	14.21148	22.00794
	0.330166	0.827807	7.029435	26.67599	40.57726
	0.590007	1.151466	7.78392	24.87446	35.54719
CLOVERDALE _05-02-10-19	0.652484	1.107858	6.279293	17.56525	22.89307
CLOVERDALE _05-03-20-19	0.714758	1.350218	6.270473	16.84026	22.3323
CLOVERDALE _511-19	0.035819	0.060508	3.585887	16.01984	22.53548
	0.03325	0.053655	3.823827	18.18751	26.42663
	0.155437	0.40441	6.122943	21.26041	29.73962
	0.250753	0.433464	5.373145	18.24098	25.48885
CARTHAGE PT_512-19	120.5243	132.9135	189.944	264.8598	288.2597
BUTLER LAKE_07-01-19	0.064732	0.166858	3.942637	16.1676	24.90974
	0.037363	0.064117	3.697117	24.5341	49.26035
	0.083904	0.262767	5.241495	19.82274	29.7965
	0.03745	0.065596	3.355678	16.35652	26.09247
BUTLER LAKE_07-02-19	0.050789	0.126292	4.633632	18.93842	29.31711
SALT LAKE_08-01-19	0.072016	0.142841	2.930431	27.99627	50.80493
	0.078241	0.163588	3.224182	38.36878	71.73459
	0.036921	0.064474	5.596796	38.41214	73.91126
	0.171621	0.45735	7.8863	41.17791	70.95165
SALT LAKE _08-02-19	0.044404	0.087501	4.222338	20.81044	33.93198
SALT LAKE _08-03-19	0.059949	0.172783	4.761585	17.70753	25.90458
SALT LAKE_08-04-19	0.104414	0.289146	5.443761	21.01754	31.9993
	0.351996	0.553239	6.06456	24.13152	39.53864
	0.115243	0.275225	4.923378	21.20558	34.22304
	0.025808	0.035697	0.865455	14.66207	23.71613
SALTLAKE_08-05-19	0.022101	0.028581	0.121627	9.03898	14.81353

Table E.1 (continued).

SIBLEY_513-19	0.772843	1.122377	9.182584	23.0112	26.76665
SIBLEY _514-19	0.041865	0.080279	7.737797	45.36545	56.78389

Table E.2 *Raw grain size values for the 2020 flood sediments.*

Site ID	D_{10}	D_{16}	D_{50}	D_{84}	D_{90}
SCCNWR_503-20	2.799091	4.121818	12.75455	52.66364	98.44545
	2.376	3.745	12.13	54.91	102.52
	2.239	3.588	10.76	33.27	55.11
	2.995	4.234	12.32	51.93	96.79
SCCNWR_058-20	1.982	3.433	10.71	31.38	45.62
	3.629	4.949	15.26	60.81	95.02
	2.423	3.716	11.3	33.64	48
	1.967	3.55	12.56	42.68	65.28
SCCNWR_059-20	2.495	3.862	11.95	39.19	64.05
	1.709	3.187	9.777	27.81	38.08
	2.989	4.315	13.58	56.35	96.94
	1.167	2.815	7.754	17.94	22.68
SCCNWR_504-20	2.602	4.411	18.08	50.55	67.91
	2.813	4.075	14.08	43.77	57.65
	2.349	4.089	16.88	47.74	63.14
	3.053	4.704	18.34	49.92	65.83
LOCHLEVEN_506-20	2.707	4.182	14.2	50.87	81.8
	2.103	3.805	13.82	54.5	94.5
	3.102	4.454	14.08	48.79	77.84
	3.044	4.34	13.27	43.07	67.88
LOCHLEVEN_505-21	3.1	4.494	14.62	40.54	52.74
	2.288	3.798	13.28	41.34	55.48
	1.476	3.059	9.132	23.3	30.24
	2.082	3.474	10.77	34.73	51.79
LOCHLEVEN_507-22	2.119	3.749	13.14	75.18	128
	2.605	3.904	12.36	44.64	73.09
	2.46	3.823	11.87	45.83	82.17
	2.744	3.954	11.74	44.58	74.26

Table E.2 (continued).

LOCHLEVEN_508-23	2.953	4.169	12.27	48.13	80.77
	2.83	4.12	13.25	58.76	91.83
	2.546	3.842	11.99	43.56	66.6
	1.886	3.383	10.68	36.21	56.39
LOCHLEVEN_509-24	2.324	3.67	11.26	31.59	42.74
	1.563	3.29	11.6	34.48	47.49
	2.346	3.769	13.46	47.63	70.64
	0.893	2.539	9.646	28.37	39.19
LOCHLEVEN_510-25	2.449	3.705	10.97	32.27	46.67
	1.4056	3.216	10.986	36.01	56.41
	2.213	3.526	10.568	29.12	40.46
	0.6433	1.758	8.501	23.82	32.32
ARTONISH_01-01-00-20	143.5	159.2	235.5	343.5	379.7
	132.9	146.4	207.5	294.4	322.9
	122.2	134.8	193.5	275.5	303
	95.52	110.9	178.3	276.5	309.2
ARTONISH_01-002-10-20	133.5	148.4	217.8	316.9	348.7
ARTONISH_01-003-20-20	35.2	61.17	147.1	257.7	296.2
ARTONISH_01-005-60-20	136.5	150.3	213	298.8	326.7
ARTONISH_01-06-80-20	103.2	115.3	166.8	236.1	259.3
ARTONISH_01-07-120-20	12.9	20.65	61.37	131.3	159
CARTHAGEPT_040-20	96.9	109.4	165.2	241	266
CLOVERDALE_04-02-10-20	3.268667	4.685333	17.29333	141.8067	205.8667
	2.87	4.19	15.03333	100.0467	149.9867
	2.959	4.172	12.98	57.17	92.53
	2.499	3.667	11.28	41.16	64.5
CLOVERDALE_04-03-20-20	2.751	3.934	11.46	39.63	61.17
CLOVERDALE_04-04-40-20	2.651	3.837	10.932	38.41	60.9
CLOVERDALE_04-05-50-20	2.995	4.254	12.7	54.61	89.29
CLOVERDALE_04-06-61-20	3.197	4.368	12.53	51.02	79.02
	2.605	3.798	11.49	41.84	63.28
	0.7125	1.361	5.624	12.3	15.15
	3.188667	4.432667	13.65333	70.59333	117.28
CLOVERDALE_04-07-80-20	3.081	4.3	12.92	59.15	93.5
CLOVERDALE_04-08-90-20	2.409	3.572	10.351	32.02	45.05
CLOVERDALE_04-09-100-20	2.8	4.021333	12.65333	61.24	101.7733

Table E.2 (continued).

CLOVERDALE_04-10-110-20	2.432	3.666667	10.57133	37.7	62
CLOVERDALE_04-11-120-20	2.301333	3.554	11.37867	55.84	88.35333
	2.013333	3.332	9.826	29.30667	43.1
	1.415333	2.994667	9.203333	26.92667	40.02667
	2.354	3.6	11.24	47.57333	75.51333
CLOVERDALE_04-12-130-20	2.617333	3.758	11.044	42.25333	67.12667
CLOVERDALE_PAD036	3.117333	4.293333	12.45333	36.44	51.48
CLOVERDALE_05-01-00B	0.942533	2.565333	9.286667	26.95333	37.54667
	2.286	3.624667	10.93333	29.22	40.35333
	2.854667	4.105333	11.80667	31.12667	42.8
	2.73	4.086667	12.68	44.41333	69.7
CLOVERDALE_05-02-10-20	1.588	3.061333	9.42	23.25333	30.15333
CLOVERDALE_05-03-20-20	2.590667	3.924	11.85333	32.69333	46.16
CLOVERDALE_511-20	2.454	3.75	11.81	32.09	42.47
	2.914667	4.173333	12.5	40.71333	73.36
	2.351	3.696	11.71	31.4	42.11
	2.551333	3.948667	12.78667	40.32	62.70667
CARTHAGE PT_512-20	106.9	128.8	214.5	332.5	371.5
BUTLER LAKE_07-01-20	1.910667	3.398	11.94	58.73333	93.72
	2.113333	3.249333	9.222667	39.60667	63.27333
	1.939333	3.19	9.156	29.78	45.72667
	2.062	3.349333	10.13533	38.16	58.68
BUTLER LAKE_07-02-20	1.733333	3.165333	9.951333	31.94667	47.44667
SALT LAKE_08-01-20	3.591333	5.013333	15.64	75.19333	132.8
	2.085	3.432	10.96	46.56	82.31
	3.3	4.729333	15.54	81.17333	138.9333
	3.969524	5.573333	19.96667	144.7619	209.9524
SALT LAKE_08-02-20	1.613333	3.23	10.63933	34.1	53.34667
SALT LAKE_08-03-20	2.412667	3.717333	11.24667	38.00667	61.21333
SALT LAKE_08-04-20	1.3046	2.994667	9.841333	28.75333	41.45333
	1.588	3.227	10.024	25.28	33.69
	0.62	1.7515	8.758	24.28	33.82
	0.8433	2.181	8.534	21.59	27.65
SALT LAKE_08-05-20	2.667	3.911	11.37	30.95	43.78
SIBLEY_513-20	2.909	4.729	28.18	75.71	101.2
SIBLEY_514-20	1.0719	2.716	8.211	21.58	29.34

APPENDIX F – RAW MAGNETIC SUSCEPTIBILITY VALUES

Table F.1 *Raw magnetic susceptibility values for the 2018- 2019 sediment samples.*

Site ID	Mass Susc. Raw Meas. in SI	Mass Susc. Meas. in SI	Correct. Factor	Correct. Offset
SCCNWR_055-19	2.41E-03	3.51E-06	1.47E-03	-3.75E-08
	3.31E-04	-5.18E-06	1.47E-03	-5.67E-06
	1.11E-03	2.79E-06	1.47E-03	1.17E-06
	1.49E-03	-2.41E-04	1.46E-03	-2.43E-04
SANDSHEET_501-19	2.80E-04	-3.10E-05	1.47E-03	-3.15E-05
SCCNWR_056-19	3.58E-04	1.63E-05	1.47E-03	1.58E-05
	3.42E-04	2.70E-05	1.47E-03	2.65E-05
	4.03E-04	5.32E-06	1.45E-03	4.73E-06
	4.05E-04	-1.78E-05	1.45E-03	-1.84E-05
SCCNWR_057-19	3.76E-04	-1.90E-05	1.47E-03	-1.95E-05
	3.69E-04	1.95E-06	1.47E-03	1.41E-06
	4.89E-04	-1.01E-04	1.47E-03	-1.02E-04
	3.20E-04	3.17E-05	1.45E-03	3.12E-05
SCCNWR_502-19	3.72E-04	7.49E-06	1.47E-03	6.94E-06
	4.74E-04	1.37E-04	1.46E-03	1.36E-04
	3.91E-04	-1.96E-05	1.47E-03	-2.02E-05
	3.82E-04	4.15E-06	1.46E-03	3.59E-06
SCCNWR_503-19	3.55E-04	-1.13E-05	1.46E-03	-1.18E-05
	3.47E-04	-1.32E-06	1.46E-03	-1.83E-06
	3.49E-04	-6.44E-07	1.46E-03	-1.15E-06
	3.38E-04	-1.04E-05	1.46E-03	-1.09E-05
SCCNWR_058-19	3.47E-04	-1.20E-05	1.47E-03	-1.25E-05
	3.29E-04	1.45E-05	1.46E-03	1.40E-05
	3.32E-04	-4.21E-06	1.47E-03	-4.70E-06
	3.69E-04	-4.99E-06	1.47E-03	-5.53E-06
SCCNWR_059-19	3.15E-04	-1.78E-06	1.45E-03	-2.24E-06
	3.27E-04	4.86E-07	1.47E-03	6.20E-09
	3.37E-04	-1.77E-05	1.47E-03	-1.82E-05
	3.34E-04	-1.99E-05	1.45E-03	-2.04E-05
SCCNWR_504-19	3.69E-04	-1.22E-05	1.47E-03	-1.28E-05
	3.94E-04	-3.49E-05	1.46E-03	-3.55E-05
	7.33E-04	-2.47E-04	1.47E-03	-2.48E-04
	3.78E-04	-9.38E-06	1.47E-03	-9.93E-06

Table F.1 (continued).

LOCHLEVEN_506-19	3.56E-04	5.52E-07	1.47E-03	2.87E-08
	3.37E-04	4.62E-07	1.46E-03	-3.03E-08
	4.97E-04	-9.66E-05	1.47E-03	-9.73E-05
	3.24E-04	3.87E-06	1.47E-03	3.40E-06
LOCHLEVEN_505-19	3.27E-04	-3.95E-07	1.47E-03	-8.75E-07
	3.37E-04	-1.74E-05	1.47E-03	-1.79E-05
	4.38E-04	-4.11E-05	1.46E-03	-4.17E-05
	3.41E-04	5.86E-06	1.46E-03	5.36E-06
LOCHLEVEN_507-19	3.28E-04	-4.55E-06	1.47E-03	-5.04E-06
	2.96E-04	-9.86E-07	1.47E-03	-1.42E-06
	5.16E-04	-1.74E-04	1.47E-03	-1.75E-04
	2.72E-04	-7.26E-06	1.47E-03	-7.66E-06
LOCHLEVEN_508-19	3.18E-04	1.16E-06	1.45E-03	6.97E-07
	2.92E-04	-1.93E-06	1.46E-03	-2.36E-06
	3.41E-04	-5.12E-06	1.46E-03	-5.61E-06
	3.39E-04	-1.83E-05	1.47E-03	-1.88E-05
LOCHLEVEN_509-19	3.19E-04	1.88E-05	1.47E-03	1.83E-05
	3.18E-04	-6.43E-06	1.47E-03	-6.90E-06
	2.81E-04	4.12E-05	1.47E-03	4.08E-05
	3.28E-04	-8.65E-06	1.46E-03	-9.13E-06
LOCHLEVEN_510-19	3.62E-04	1.02E-05	1.47E-03	9.63E-06
	3.45E-04	-3.60E-06	1.47E-03	-4.10E-06
	3.29E-04	-7.69E-06	1.46E-03	-8.17E-06
	3.00E-04	3.60E-05	1.46E-03	3.56E-05
ARTONISH_01-01-00-19	1.70E-03	-1.03E-05	1.47E-03	-1.28E-05
	6.14E-04	2.00E-06	1.47E-03	1.10E-06
	7.43E-04	-6.95E-06	1.47E-03	-8.05E-06
	1.51E-03	4.41E-08	1.44E-03	-2.14E-06
ARTONISH _01-002-10-19	3.45E-04	1.63E-06	1.47E-03	1.12E-06
	3.93E-04	-6.47E-05	1.47E-03	-6.53E-05
ARTONISH _01-003-20-19	4.60E-04	-1.22E-05	1.47E-03	-1.29E-05
ARTONISH _01-005-60-19	2.63E-04	2.28E-06	1.47E-03	1.89E-06
ARTONISH _01-06-80-19	2.27E-04	-2.92E-08	1.46E-03	-3.59E-07

Table F.1 (continued).

ARTONISH _01-07-120-19	3.50E-04	8.65E-06	1.47E-03	8.14E-06
	3.06E-04	1.76E-06	1.47E-03	1.31E-06
	3.86E-04	-1.05E-05	1.46E-03	-1.11E-05
	3.19E-04	5.18E-06	1.47E-03	4.71E-06
CARTHAGE PT_040-19	1.31E-03	1.93E-05	1.46E-03	1.74E-05
CLOVERDALE_04-02-10-19	3.22E-04	2.15E-05	1.46E-03	2.10E-05
	2.94E-04	1.59E-05	1.47E-03	1.54E-05
	3.71E-04	3.13E-05	1.47E-03	3.08E-05
	1.30E-03	-6.03E-04	1.47E-03	-6.05E-04
CLOVERDALE _04-03-20-19	3.42E-04	-1.71E-04	1.46E-03	-1.71E-04
CLOVERDALE_04-04-40-19	3.10E-04	-1.41E-05	1.47E-03	-1.45E-05
CLOVERDALE _04-05-50-19	3.02E-04	-1.25E-05	1.46E-03	-1.29E-05
CLOVERDALE _04-06-61-19	3.03E-04	3.86E-06	1.47E-03	3.41E-06
	3.62E-04	-4.07E-05	1.46E-03	-4.13E-05
	3.40E-04	-5.72E-06	1.45E-03	-6.21E-06
	3.59E-04	-7.68E-06	1.46E-03	-8.21E-06
CLOVERDALE _04-07-80-19	2.53E-04	1.20E-05	1.47E-03	1.16E-05
CLOVERDALE _04-08-90-19	3.52E-04	-6.64E-05	1.46E-03	-6.69E-05
CLOVERDALE _04-09-100-19	3.43E-04	1.35E-06	1.46E-03	8.49E-07
CLOVERDALE _04-10-110-19	3.87E-04	-2.15E-05	1.45E-03	-2.20E-05
CLOVERDALE_04-11-120-19	8.74E-04	-1.22E-04	1.46E-03	-1.24E-04
	2.09E-04	1.02E-04	1.46E-03	1.02E-04
	4.39E-04	-1.02E-04	1.47E-03	-1.03E-04
	3.68E-04	-1.46E-05	1.46E-03	-1.51E-05
CLOVERDALE _04-12-130-19	3.37E-04	1.81E-05	1.46E-03	1.76E-05
CLOVERDALE _PAD036	6.23E-04	-1.15E-04	1.46E-03	-1.16E-04

Table F.1 (continued).

CLOVERDALE _05-01-00B	3.14E-04	1.64E-05	1.47E-03	1.59E-05
	2.86E-04	3.44E-06	1.47E-03	3.02E-06
	3.22E-04	-4.29E-05	1.47E-03	-4.34E-05
	3.21E-04	-1.22E-06	1.47E-03	-1.70E-06
CLOVERDALE _05-02-10-19	3.41E-04	1.78E-06	1.47E-03	1.28E-06
CLOVERDALE _05-03-20-19	3.65E-04	-5.05E-06	1.46E-03	-5.58E-06
CLOVERDALE _511-19	3.25E-04	2.67E-05	1.47E-03	2.63E-05
	3.82E-04	-5.76E-05	1.45E-03	-5.81E-05
	6.81E-04	-3.65E-04	1.45E-03	-3.66E-04
	3.03E-04	4.35E-05	1.47E-03	4.30E-05
CARTHAGE PT_512-19	3.21E-04	-3.06E-05	1.46E-03	-3.11E-05
BUTLER LAKE_07-01-19	3.50E-04	-1.18E-04	1.47E-03	-1.19E-04
	3.54E-04	-3.32E-08	1.46E-03	-5.50E-07
	2.98E-04	1.85E-05	1.47E-03	1.80E-05
	3.41E-04	-1.73E-04	1.45E-03	-1.73E-04
BUTLER LAKE_07-02-19	2.94E-04	5.55E-05	1.46E-03	5.51E-05
SALT LAKE_08-01-19	3.80E-04	-4.52E-05	1.47E-03	-4.57E-05
	3.15E-04	-1.78E-05	1.47E-03	-1.83E-05
	3.15E-04	-2.83E-05	1.47E-03	-2.87E-05
	3.39E-04	-1.01E-03	1.46E-03	-1.01E-03
SALT LAKE _08-02-19	3.12E-04	-5.22E-06	1.47E-03	-5.67E-06
SALT LAKE _08-03-19	3.72E-04	-2.62E-06	1.46E-03	-3.16E-06
SALT LAKE_08-04-19	3.62E-04	2.02E-05	1.46E-03	1.97E-05
	3.47E-04	-5.26E-06	1.47E-03	-5.77E-06
	2.92E-04	1.30E-05	1.47E-03	1.26E-05
	5.91E-04	-5.47E-05	1.45E-03	-5.55E-05
SALTLAKE_08-05-19	3.08E-04	-3.32E-05	1.46E-03	-3.37E-05
SIBLEY_513-19	4.70E-04	-1.04E-04	1.45E-03	-1.05E-04
SIBLEY _514-19	3.20E-04	3.41E-06	1.47E-03	2.94E-06

Table F.2 *Raw magnetic susceptibility values for the 2020 sediment samples.*

Site ID	Mass Susc. Raw Meas. in SI	Mass Susc. Meas. in SI	Correct. Factor	Correct. Offset
SCCNWR_503-20	3.38E-04	1.21E-05	1.46E-03	1.17E-05
	3.49E-04	-1.77E-04	1.46E-03	-1.77E-04
	3.55E-04	-3.54E-05	1.47E-03	-3.59E-05
	2.76E-04	7.47E-07	1.47E-03	3.41E-07
SCCNWR_058-20	7.48E-05	2.48E-04	1.47E-03	2.48E-04
	3.86E-04	-6.11E-05	1.46E-03	-6.17E-05
	3.76E-04	-1.29E-04	1.46E-03	-1.30E-04
	3.70E-04	-1.13E-04	1.47E-03	-1.14E-04
SCCNWR_059-20	3.16E-04	-2.16E-04	1.46E-03	-2.16E-04
	7.67E-05	7.75E-04	1.46E-03	7.75E-04
	3.57E-04	4.74E-05	1.46E-03	4.68E-05
	-1.64E-03	1.10E-03	1.46E-03	1.10E-03
SCCNWR_504-20	3.57E-03	-1.86E-03	1.46E-03	-1.86E-03
	4.51E-04	-1.82E-05	1.47E-03	-1.89E-05
	3.58E-04	6.36E-06	1.46E-03	5.84E-06
	3.17E-04	4.02E-04	1.46E-03	4.01E-04
LOCHLEVEN_506-20	2.97E-04	6.98E-05	1.47E-03	6.93E-05
	1.12E-03	-5.33E-04	1.46E-03	-5.35E-04
	2.55E-04	-1.44E-05	1.46E-03	-1.48E-05
	1.55E-04	1.73E-04	1.47E-03	1.73E-04
LOCHLEVEN_505-20	1.92E-04	-2.68E-04	1.46E-03	-2.68E-04
	3.65E-04	-6.16E-06	1.46E-03	-6.69E-06
	2.47E-04	3.73E-05	1.45E-03	3.69E-05
	3.04E-04	3.80E-05	1.47E-03	3.75E-05
LOCHLEVEN_507-20	-3.84E-04	6.94E-04	1.47E-03	6.94E-04
	2.74E-04	-3.06E-04	1.46E-03	-3.06E-04
	-6.63E-06	2.19E-04	1.46E-03	2.19E-04
	8.31E-04	-2.47E-04	1.47E-03	-2.48E-04
LOCHLEVEN_508-20	6.60E-04	3.03E-04	1.46E-03	3.02E-04
	5.82E-04	-1.81E-04	1.45E-03	-1.82E-04
	5.00E-04	-8.09E-06	1.46E-03	-8.82E-06

Table F.2 (continued).

LOCHLEVEN_509-20	-9.63E-04	8.96E-04	1.46E-03	8.97E-04
	3.72E-04	4.43E-05	1.46E-03	4.37E-05
	6.08E-04	-1.58E-04	1.46E-03	-1.59E-04
	3.55E-04	-2.89E-06	1.46E-03	-3.41E-06
LOCHLEVEN_510-20	3.22E-04	-1.38E-04	1.46E-03	-1.39E-04
	3.09E-04	1.91E-05	1.47E-03	1.86E-05
	1.12E-04	1.47E-04	1.45E-03	1.47E-04
	3.41E-04	-3.00E-04	1.47E-03	-3.01E-04
ARTONISH_01-01-00-20	7.04E-04	3.21E-06	1.47E-03	2.18E-06
	3.91E-04	-2.78E-05	3.36E-04	-2.79E-05
	6.03E-04	-3.53E-05	1.47E-03	-3.62E-05
	1.24E-03	-1.87E-05	1.47E-03	-2.05E-05
ARTONISH_01-002-10-20	5.41E-04	1.58E-05	1.46E-03	1.50E-05
ARTONISH_01-003-20-20	7.00E-04	-8.97E-06	1.47E-03	-1.00E-05
ARTONISH_01-005-60-20	6.32E-04	-2.79E-04	1.46E-03	-2.80E-04
ARTONISH_01-06-80-20	3.30E-04	1.57E-05	1.46E-03	1.52E-05
ARTONISH_01-07-120-20	3.99E-04	1.30E-04	1.45E-03	1.29E-04
CARTHAGEPT_040-20	9.24E-04	-1.89E-05	1.46E-03	-2.02E-05
CLOVERDALE_04-02-10-20	8.46E-04	-2.67E-04	1.46E-03	-2.69E-04
	9.65E-04	-3.65E-04	1.47E-03	-3.67E-04
	4.29E-04	-6.99E-05	1.46E-03	-7.05E-05
	3.33E-04	-3.08E-06	1.46E-03	-3.56E-06
CLOVERDALE_04-03-20-20	3.52E-04	-1.97E-04	1.47E-03	-1.98E-04
CLOVERDALE_04-04-40-20	1.19E-03	1.17E-03	1.47E-03	1.17E-03
CLOVERDALE_04-05-50-20	3.15E-04	1.98E-05	1.47E-03	1.94E-05
CLOVERDALE_04-06-61-20	3.96E-04	-1.32E-04	1.47E-03	-1.33E-04
	4.13E-04	-5.10E-05	1.47E-03	-5.16E-05
	-1.40E-04	-2.02E-04	1.46E-03	-2.02E-04
	-5.82E-03	3.48E-03	1.46E-03	3.49E-03
CLOVERDALE_04-07-80-20	6.38E-04	-9.47E-05	1.47E-03	-9.56E-05
CLOVERDALE_04-08-90-20	8.33E-04	-3.58E-04	1.47E-03	-3.60E-04
CLOVERDALE_04-09-100-20	6.15E-04	-1.42E-04	1.47E-03	-1.43E-04
CLOVERDALE_04-10-110-20	3.99E-04	-1.10E-05	1.46E-03	-1.16E-05

Table F.2 (continued).

CLOVERDALE_04-11-120-20	3.29E-04	2.20E-05	1.47E-03	2.15E-05
	4.15E-04	-2.40E-05	1.46E-03	-2.46E-05
	5.47E-04	-1.40E-04	1.45E-03	-1.41E-04
	5.48E-04	-1.27E-04	1.46E-03	-1.28E-04
CLOVERDALE_04-12-130-20	2.80E-04	3.19E-05	1.46E-03	3.15E-05
CLOVERDALE_PAD036	1.55E-03	-6.20E-04	1.46E-03	-6.22E-04
CLOVERDALE_05-01-00B	4.12E-04	-6.94E-05	1.47E-03	-7.00E-05
	2.20E-04	-1.71E-04	1.46E-03	-1.71E-04
	9.42E-04	-6.14E-04	1.45E-03	-6.16E-04
	3.33E-04	-3.53E-05	1.47E-03	-3.58E-05
CLOVERDALE_05-02-10-20	3.10E-04	-1.80E-05	1.46E-03	-1.85E-05
CLOVERDALE_05-03-20-20	4.46E-04	-8.36E-05	1.46E-03	-8.43E-05
CLOVERDALE_511-20	5.38E-04	-1.41E-04	1.47E-03	-1.42E-04
	2.96E-04	9.84E-05	1.45E-03	9.79E-05
	1.60E-03	-7.89E-04	1.47E-03	-7.91E-04
	2.94E-04	-1.60E-05	1.46E-03	-1.65E-05
CARTHAGE PT_512-20	1.11E-03	-4.75E-05	1.47E-03	-4.92E-05
BUTLER LAKE_07-01-20	3.19E-04	-1.10E-05	1.46E-03	-1.15E-05
	4.03E-04	-3.99E-05	1.47E-03	-4.05E-05
BUTLER LAKE_07-02-20	4.34E-04	-3.23E-05	1.46E-03	-3.29E-05
SALT LAKE_08-01-20	6.17E-04	-7.08E-04	1.47E-03	-7.09E-04
	-6.54E-05	6.28E-05	1.46E-03	6.29E-05
	3.32E-04	-1.74E-05	1.45E-03	-1.79E-05
	3.84E-04	-5.18E-04	1.47E-03	-5.19E-04
SALT LAKE_08-02-20	-2.47E-04	3.03E-04	1.47E-03	3.04E-04
SALT LAKE_08-03-20	8.09E-04	-2.43E-04	1.45E-03	-2.44E-04
SALT LAKE_08-04-20	3.32E-04	-1.54E-06	1.47E-03	-2.02E-06
	3.65E-04	-1.36E-05	1.45E-03	-1.41E-05
	5.36E-04	-1.71E-04	1.45E-03	-1.72E-04
	6.91E-04	-7.22E-05	1.46E-03	-7.32E-05
SALT LAKE_08-05-23	-3.70E-05	5.48E-04	1.45E-03	5.49E-04
SIBLEY_513-20	3.68E-04	1.70E-05	1.47E-03	1.65E-05
SIBLEY_514-20	3.56E-04	-8.72E-06	1.46E-03	-9.24E-06

REFERENCES

Allison, M.A., and Meselhe, E.H., 2010, The use of large water and sediment diversions in the lower Mississippi River (Louisiana) for coastal restoration, Journal of Hydrology, 387, 346-360.

Aslan, A., and Autin, W. J., 1999, Evolution of the Holocene Mississippi River floodplain, Ferriday, Louisiana; Insights on the origin of fine- grained floodplains, Journal of Sedimentary Research, Vol. 69, No. 4, p. 800-815.

Asselman, N. E. M., and Middelkoop, H., 1995, Floodplain sedimentation: quantities, patterns and processes, Earth surface Processes and Landforms, vol. 20, p. 481-499.

Asselman, N. E. M., and Middelkoop, H., 1998, Temporal variability of contemporary floodplain sedimentation in the Rhine Meuse delta, the Netherlands, Earth Surface Processes and Landforms, vol. 23, p. 595-609.

Benke, A.C., Chaubey, I., Milton Ward, G., Lloyd Dunn, E., Flood pulse dynamics of an unregulated river floodplain in the southeastern U.S. coastal plain, Ecology, v. 81, i. 10, p. 2730-2741.

Blum, M.D., and Roberts, H.H., 2009, Drowning of the Mississippi Delta due to insufficient sediment supply and global sea-level rise, Nature Geoscience, vol. 2, p. 488-491.

Bridge, J.S., 2003, Rivers and floodplains; forms processes, and sedimentary record: Oxford, Blackwell Publishing, 491 p.

Brown, J.B., Sprague, L.A., and Dupree, J.A., 2011, Nutrient sources and transport in the Missouri River Basin, with Emphasis on the Effects of Irrigation and Reservoirs, Journal of the American Water Resources Association, 47(5): 1034-1060.

Charlton, R., 2008, Fundamentals of Fluvial Geomorphology: New York, Routledge, p. 234.

Fisk, H. N., 1944, Geological investigation of the alluvial valley of the lower Mississippi river, War Department, Corps of Engineers, Washington DC, p.78.

Heimann, D.C., Sprague, L.A., and Blevins, D.W., 2011, Trends in suspended-sediment loads and concentrations in the Mississippi River Basin, 1950–2009: U.S. Geological Survey Scientific Investigations Report 2011–5200, p. 33.

Heitmuller, F.T., Hudson, P.F., and Kesel, R.H., 2017. Overbank sedimentation from the historic A.D. 2011 flood along the Lower Mississippi River, USA. Geology, v. 45. No. 2. P. 107-110.

Hudson, P.F., and Kesel, R.H., 2000, Relationships between lateral migration rates and channel

geometry in the Lower Mississippi River, Geology 28, 531-534.

Hudson, P.F. and Heitmuller, F.T. 2003. Local- and watershed-scale controls on the spatial

variability of natural levee deposits in a large fine-grained floodplain: Lower Pánuco basin, Mexico. Geomorphology 56, p. 255-269.

Kaase, C.T., Kupfer, J.A., 2016, Sedimentation patterns across a Coastal Plain floodplain: The importance of hydrogeomorphic influences and cross-floodplain connectivity, Geomorphology, 269, 43-55.

Kesel, R.H., Dunne, K.C., McDonald, R.C., Allison, K.R., and Spicer, B.E., 1974, Lateral erosion and overbank deposition on the Mississippi River in Louisiana caused by 1973 flooding: Geology, v. 2, p. 461–464

Middelkoop, H., and Asselman, N.E.M., 1998, Spatial variability of floodplain sedimentation at the event scale in the Rhine-Meuse delta, The Netherlands, The Journal of the British Society for Geomorphology, v. 23, no. 6, p. 561-573.

Meade, R. H., and Moody, J.A., 2010, Causes for the decline of suspended-sediment discharge in the Mississippi River system, 1940-2007, Hydrological Processes, v. 24., p. 35-49.

Nittrouer, J.A., Shaw, J., Lamb, M.P., and Mohrig, D., 2012, Spatial and temporal trends for water flow velocity and bed-material sediment transport in the lower Mississippi River, GSA Bulletin 124 (3-4): p. 400-414.

Noe G.B., Hupp C.R., 2005. Carbon, nitrogen, and phosphorus accumulation in floodplains of Atlantic Coastal Plain rivers, USA. Ecological Applications 15:1178-90.

Noe G.B., Hupp C.R., 2009. Retention of riverine sediment nutrient loads by Coastal Plain floodplains. Ecosystems 12:728-46

Noe G.B., Hupp C.R., and Rybicki N.B., 2013. Hydrogeomorphology Influences Soil Nitrogen and Phosphorus Mineralization in Floodplain Wetlands. Ecosystems 16: 75-94

Ochs C.A., Shields F.D. Jr. 2019. Fluxes of nutrients and primary production between the main channel and floodplain backwaters of the Lower Mississippi River –

Development of a simulation model. River Research and Applications. 35: 979-988.

Pizzuto, J. E., 1987, Sediment diffusion during overbank flows, The Journal of the International Association of Sedimentologists, v. 34, i. 2, p. 301-317.

Pongrukam, O, Ochs, CA. 2015. The rise and fall of the Lower Mississippi: Effects of hydrologic connection on floodplain backwaters. Hydrobiologia. 742: 169-183.

RStudio Team (2020). RStudio: Integrated Development for R. RStudio, PBC, Boston, MA URL http://www.rstudio.com.

Rus, D.L., Galloway, J.M., and Alexander, J.S., 2015, Characteristics of sediment transport at selected sites along the Missouri River, 2011-12, US Geological Survey Scientific Investigations Report 2015-5127, p.34.

Saucier, R.T., 1994, Geomorphology and Quaternary geologic history of the Lower Mississippi River valley: Vicksburg, Mississippi, U.S. Army Corps of Engineers, Mississippi River Commission, 364 p.

Schönbrunner, I.M., Preiner, S., and Hein, T., 2012, Impact of drying and re-flooding of sediment on phosphorus dynamics of river-floodplain systems, Science of the Total Environment, vol. 432, p. 329-337.

Schramm, H.L. Jr., Cox, M.S., Tietjen, T.E., and Ezell, A.W., 2009. Nutrient dynamics in the Lower Mississippi River floodplain: Comparing present and historic hydrologic conditions. Wetlands, 29: 476-487.

Spink, A., Sparks, R.E., Van Oorschot M., and Verhoeven, J.T.A., 1998, Nutrient Dynamics of Large River Floodplains. Regulated Rivers: Research & Management. 14: 203-216.

Stone, M.C., Byrne, C.F., and Morrison, R.R., Evaluating the impacts of hydrologic and geomorphic alterations on floodplain connectivity. 2017. Ecohydrology. 10:e1833.

Tockner, K., Pennetzdorfer, D., Reiner, N., Schiemer, F., and Ward, J.V., 1999, Hydrological connectivity, and the exchange of organic matter and nutrients in a dynamic river- floodplain system (Danube, Austria), Freshwater Biology. 41: 521-535

Tockner, K., Pusch, M., Borchardt, D., Lorang, M.S., 2010, Multiple stressors in couples river- floodplain ecosystems, Freshwater Biology, 55: 135-151.

U.S. Geological Survey, 2022, Water Quality Samples for the Nation: https://nwis.waterdata.usgs.gov/nwis/qw (accessed May 2022).